Chemical Geology 581 (2021) 120416

Contents lists available at ScienceDirect

Chemical Geology

journal homepage: www.elsevier.com/locate/chemgeo

The impact of primary processes and secondary alteration on the stable isotope composition of ocean island basalts

Richard M. Gaschnig [a,*], Christopher T. Reinhard [b], Noah J. Planavsky [c], Xiangli Wang [d], Dan Asael [c], Matthew G. Jackson [e]

[a] Dept of Environmental, Earth and Atmospheric Sciences, University of Massachusetts Lowell. 1 University Ave, Lowell, MA 01854, United States of America
[b] School of Earth and Atmospheric Sciences, Georgia Institute of Technology, United States of America
[c] Dept of Earth and Planetary Sciences, Yale University, United States of America
[d] Dept of Marine Sciences, University of South Alabama, United States of America
[e] Dept of Earth Science, University of California, Santa Barbara, United States of America

ARTICLE INFO

Editor: Catherine Chauvel

Keywords:
OIB
Molybdenum isotopes
Uranium isotopes
Mantle

ABSTRACT

Molybdenum and uranium are redox sensitive elements that experience isotope fractionation in the Earth-surface environment. Recent studies have explored the transfer of these fractionated signals in subduction zones to arc magmas, but less is known about the full variation of these isotopic tracers in the mantle, particularly domains of the mantle that may feed hot spots. Here, we present Mo and U isotope data for lava samples from Pitcairn, the Samoan Islands, and St. Helena, representing classic localities for the EM-1 (enriched mantle 1), EM-2 (enriched mantle 2) and HIMU (high μ, where μ is $^{238}U/^{204}Pb$) endmembers.

Mo and U isotope compositions are highly variable for each location, and the range of variation largely overlaps between the three localities. However, some of this variation may be attributable to chemical weathering and low-temperature alteration effects, as revealed by $^{234}U/^{238}U$ disequilibrium, also reported here; many samples, especially from Pitcairn, have a ^{234}U deficit, while a few others have a ^{234}U excess. Samples with the greatest ^{234}U deficit tend to have the highest Ce/Mo for a given locality and samples with the lowest $\delta^{98}Mo$ typically show considerable $^{234}U/^{238}U$ disequilibrium, suggesting that Mo was leached during weathering with preferential loss of heavy isotopes.

Of the samples with ^{234}U and ^{238}U activity in equilibrium from the three localities, most have $\delta^{98}Mo$ values lower than the published average for MORB, but they have $\delta^{238}U$ values within uncertainty of MORB. In contrast, two Samoan samples have $\delta^{98}Mo$ values similar to MORB but have isotopically light $\delta^{238}U$. While the low $\delta^{98}Mo$ seen in many samples could be attributable to the incorporation of subducted sediments into the plume sources, such sediment would have needed to be deposited under oxic oceanographic conditions that were not prevalent until the Neoproterozoic; in contrast, radiogenic isotope compositions tend to point towards a much greater age of recycled components in the plume sources. Instead, we consider the most likely cause of the light Mo isotope compositions to be incorporation into the source region of ancient subducted ocean crust that experienced Mo isotope fractionation during devolatilization, which favored loss of the heavy isotopes, as has been proposed in several recent studies. This is in line with models for the origin of the EM-1 and HIMU source, along with a portion of the Samoan source. The two Samoan samples with isotopically light U, but MORB-like $\delta^{98}Mo$, may reflect influence of a distinct pool of mid-Proterozoic recycled ocean crust.

1. Introduction

The operation of plate tectonics on likely multi-billion-year timescales has led to the widespread pollution of the Earth's mantle with materials that have experienced low-temperature interaction with the Earth's hydrosphere and atmosphere (Allègre et al., 1980). Other processes such as delamination of continental lithosphere may also contribute to mantle chemical heterogeneity (Arndt and Goldstein, 1989; Kay and Mahlburg-Kay, 1991). It is also possible that preserved zones of primitive mantle, chemically unmodified since shortly after

* Corresponding author.
E-mail address: richard_gaschnig@uml.edu (R.M. Gaschnig).

https://doi.org/10.1016/j.chemgeo.2021.120416
Received 15 February 2021; Received in revised form 17 June 2021; Accepted 1 July 2021
Available online 3 July 2021

core segregation, also exist (Willbold and Stracke, 2010). The main sources of information on chemical heterogeneities in the mantle are mafic lavas erupted in the ocean basins, where shallow-level contamination by continental crust is not a concern. Midocean ridge basalts (MORBs) are generally thought to sample the ambient convecting upper mantle, and while chemical heterogeneities between ridges in different ocean basins exist, the magnitude of these variations, particularly for radiogenic isotopes, is less than that seen in ocean island basalts (OIBs) erupted at hot spots (Hart et al., 1992; Hofmann, 1997; White, 1985, 2010). OIBs are usually interpreted to be derived from buoyantly upwelling mantle plumes carrying material from distinct chemical domains in the deeper mantle, and they show substantial compositional diversity with regards to radiogenic isotopes. In particular, covariation between Sr, Nd, and Pb isotopes suggest that most OIBs can be explained by mixing between a series of extreme end member compositions (Zindler and Hart, 1986).

Stracke et al. (2005) used the term "zoo" to describe the multiple acronym-defining mantle end members described by radiogenic isotope variations in OIBs. Members of the mantle zoo that are of interest in this contribution are enriched mantle I (EM-I), enriched mantle II (EM-II), and high μ (HIMU) (White, 1985; Zindler and Hart, 1986). EM-I is characterized by moderately radiogenic Sr, unradiogenic Nd, low $^{206}Pb/^{204}Pb$, and moderately high $^{208}Pb/^{204}Pb$ at a given $^{206}Pb/^{204}Pb$, and these compositions are exemplified by OIB from the Pitcairn hotspot (Eisele et al., 2002; Garapić et al., 2015; Woodhead and McCulloch, 1989; White, 1985). A mix of subducted ocean crust and sediment, delaminated continental lower crust and/or lithosphere, and old mantle wedge material are amongst the proposed possible identities of the EM-1 source (Delavault et al., 2016; Eisele et al., 2002; Kimura et al., 2016; Willbold and Stracke, 2010; Garapić et al., 2015). EM-II is characterized by anomalously radiogenic Sr, unradiogenic Nd, and moderate $^{206}Pb/^{204}Pb$ and is exemplified by OIB from the Samoan hotspot (e.g., Zindler and Hart, 1986; Workman et al., 2004; Jackson et al., 2007a). Ancient subducted terrigenous sediment is considered to be the most likely identity of the EM-II source (e.g., Jackson et al., 2007a; White and Hofmann, 1982; Workman et al., 2008). HIMU is characterized by unradiogenic Sr, moderately radiogenic Nd, and anomalously high $^{206}Pb/^{204}Pb$, requiring a high time-integrated $^{238}U/^{204}Pb$ (i.e., high μ). The key OIB localities exhibiting this composition are St. Helena and several volcanoes in the Cook-Austral Islands (e.g., White, 1985; Chauvel et al., 1992; Woodhead, 1996). Many workers have argued that the HIMU source represents subducted altered ocean crust (Chase, 1981) that may have underwent chemical modification of the U-Th-Pb system during subduction-related dehydration (Chauvel et al., 1992; Stracke et al., 2003), although other ingredients, such as subducted marine carbonate (Castillo, 2015), or carbonatite metasomatized subcontinental lithospheric mantle (Weiss et al., 2016), have also been proposed.

The use of OIB samples to explore the composition and long-term history of different mantle domains is predicated on access to samples that have not been chemically altered by surface processes. The high glass content of many basalts and the location of most key OIB localities in warm, wet climates make these materials particularly vulnerable to chemical weathering and submarine samples are obviously vulnerable to reaction with seawater. While leaching during subaerial chemical weathering will not alter radiogenic isotope compositions, it may fractionate various metal stable isotope ratios (e.g., Wiederhold et al., 2007; Teng et al., 2010; Liu et al., 2014; Greaney et al., 2021).

This contributions reports Mo and U isotope compositions of lavas from three classic OIB localities: Samoa, Pitcairn, and St. Helena. As Mo and U are highly soluble under oxidizing weathering conditions and Mo is known to experience isotope fractionation during weathering (e.g., Pearce et al., 2010; Voegelin et al., 2012), alteration of samples is a major concern. $^{234}U/^{238}U$ disequilibrium provides a means of recognizing otherwise cryptic alteration (e.g, Andersen et al., 2015), and we consider the relationship between this parameter and Mo and $^{238}U/^{235}U$ isotope compositions. We then consider the significance of lower-than-MORB $\delta^{98}Mo$ and $\delta^{238}U$ compositions in unaltered samples.

2. Background

2.1. The Mo isotope system

Molybdenum is a redox-sensitive metal capable of forming 4+ and 6+ species, which are present in natural environments in compounds with markedly different solubilities. Weathering of continent crust under oxidizing conditions transports Mo(VI) to the oceans primarily as a soluble oxyanion species. The main mechanism for removal of Mo(VI) from seawater is via scavenging by Mn-oxide particles in oxic sedimentary environments and reduction to insoluble and particle-reactive Mo(IV) and incorporation into sediments in anoxic environments. The first process is the main driver of Mo isotope fractionation in the Earth surface environment (Kendall et al., 2017).

Mo isotopes are reported in $\delta^{98}Mo$ ($[\delta^{98}Mo = (^{98}Mo/^{95}Mo$ sample / $^{98}Mo/^{95}Mo$ standard) – 1] x 1000). Goldberg et al. (2013) recommended reporting Mo isotope data relative to the NIST-3134 standard (i.e., with the standard set to 0‰), and the majority of studies of Mo isotopes in high temperature systems have followed this approach. As mentioned above, the largest source of isotope fractionation of Mo is the scavenging of Mo(VI) by sediments in oxic depositional environments. In these environments, lighter isotopes are strongly enriched in the sediments relative to seawater (Barling and Anbar, 2004; Barling et al., 2001). Non-quantitative reduction of Mo(VI) to Mo(IV) in more oxygen poor environments can also cause isotope fractionation in the same direction (Barling et al., 2001; Azrieli-Tal et al., 2014). Alteration of ocean crust by seawater may impart it with $\delta^{98}Mo$ values higher than unaltered crust, although far less data is available (Freymuth et al., 2015; McManus et al., 2002).

The use of Mo isotopes in studies of igneous systems has surged in recent years. Bezard et al. (2016) conducted a survey of MORB lavas; all but three samples show a narrow range of Mo isotope compositions within quoted uncertainties, yielding an average of -0.16 ± 0.09‰ if one excludes the three outliers. Liang et al. (2017) reported MORB $\delta^{98}Mo$ values clustered around 0‰, but McCoy-West et al. (2019) were unable to reproduce these and reported MORB values consistent with those of Bezard et al. (2016). Studies of arc lavas have shown great isotopic variability (Casalini et al., 2019; Freymuth et al., 2016; Freymuth et al., 2015; Gaschnig et al., 2017; König et al., 2016; Voegelin et al., 2014; Willbold and Elliott, 2017; Wille et al., 2018; Villalobos-Orchard et al., 2020); many localities have yielded $\delta^{98}Mo$ values higher than MORB, including values greater than 0‰. The effects of fractional crystallization on Mo isotope ratios appear to be negligible in dry tholeiitic systems (Yang et al., 2015; Gaschnig et al., 2021), but fractional crystallization of hydrous phases such as biotite and amphibole appears to drive remaining melts to somewhat heavier isotope compositions (Voegelin et al., 2014; Wille et al., 2018; Yang et al., 2017). However, most arc studies have concluded that these effects on isotope composition are subordinate to the influence of differing slab-derived components (Freymuth et al., 2015; Freymuth et al., 2016; König et al., 2016; Gaschnig et al., 2017; Casalini et al., 2019). In order to explain the heavier-than-MORB isotope compositions in many arcs, several workers have argued that slab-derived fluids preferentially remove heavy isotopes while lighter isotopes are retained in a residual phase such as rutile or sulfide (Casalini et al., 2019; Freymuth et al., 2015; König et al., 2016; Skora et al., 2017; Willbold and Elliott, 2017), although in a few cases, unique subducting lithologies with heavy isotope signatures such as black shales may also be responsible (Freymuth et al., 2015; Gaschnig et al., 2017). An important implication of isotope fractionation by slab-derived fluids is that the residual phases in the slab will carry isotopically light Mo deeper into the mantle where it may later be sampled in OIBs. Evidence supporting this model was provided recently by Chen et al. (2019), who reported light isotope compositions in previously subducted blueschist and eclogite samples.

Table 1
Mo and U isotope results for lavas from there OIB localities.

Sample Name	Location	Approximate latitu	Approximate longi	Approximate age	Reference for radiogenic isotopic data and ages	δ^{98}Mo (‰	2 se	[Mo] (ppm)	δ^{238}U (‰)	2 se	(234U/238U)	2SE	δ^{234}U (‰)	[U] (ppm)	SiO2 (wt%)	MgO (wt%)	Mg#	LOI (wt%)	CIA	W	Ce/Mo	Th/Rb	Th/U	$^{87}Sr/^{86}Sr$	$^{143}Nd/^{144}Nd$	206Pb/204Pb	207Pb/204Pb	208Pb/204Pb
ALIA-115-03	Samoa	14.090	172.898	5 Ma	Jackson et al (2007a)	-0.49	0.09	1.10	-0.23	0.08	1.007	0.002	7	1.69	49.16	7.97	59	1.90	37	11	95	0.086	4.21	0.711409	0.512593	19.011	15.633	39.347
ALIA-115-18	Samoa	14.090	172.898	5 Ma	Jackson et al (2007a)	-0.52	0.09	1.01	-0.29	0.07	0.810	0.002	-190	1.86	52.28	5.09	56	4.40	41	14	129	0.110	5.76	0.718592	0.512314	18.957	15.643	39.399
ALIA-115-21	Samoa	14.090	172.898	5 Ma	Jackson et al (2007a)	-0.30	0.08	1.57	-0.23	0.07	0.995	0.002	-5	2.84	57.2	3.61	55	4.88	47	21	98	0.112	6.15	0.720469	0.512287	18.954	15.646	39.424
AVON3-78-1	Samoa	14.623	169.726	< 8 Ka	Workman et al. (2004)	-0.10	0.07	1.53	-0.38	0.06	1.002	0.001	2	1.06	45.5	19.7	75		32	7	48	0.144	5.68	0.708901	0.512521	19.237	15.647	39.862
OFU-04-03	Samoa - Ofu	14.2	-169.6	< 0.3 Ma	Jackson et al (2007b) for isotopes, Hart and Jas	-0.19	0.08	1.11	-0.48	0.07	1.002	0.001	2	0.72	45.0	14.7	66	2.01	32	7	57	0.119	4.54	0.704756	0.512811	19.257	15.591	39.418
T33	Samoa - Tāʻū	14.216	169.442	< 0.3 Ma	Workman et al. (2004)	-0.25	0.07	1.12	-0.25	0.10	1.000	0.003	0	0.61	47.3	12.4	66		30	5	45	0.180	4.68	0.704736	0.512780	19.284	15.596	39.445
SI6	Samoa - Savaiʻi	13.477	172.395	0.3 Ma	Workman et al. (2004)			1.37	-0.14	0.06	0.979	0.002	-21	0.93	47.2	6.6	50		42	9	57	0.083	4.75	0.706296	0.512705	18.865	15.595	39.089
Pit-1	Pitcairn	-25.071	-130.116	1.0–0.4 Ma	Garapic et al. (2015)	-0.44	0.08	1.51	-0.40	0.05	0.984	0.002	-16	0.89	48.1	7.1	56		43	9	65	0.203	7.41	0.705243	0.512447	17.630	15.460	38.936
Pit-3	Pitcairn	-25.071	-130.116	1.0–0.4 Ma	Garapic et al. (2015)	-0.39	0.06	1.58	-0.22	0.05	0.991	0.001	-9	1.24	48.7	7.8	57		42	9	66	0.243	6.18	0.705220	0.512435	17.611	15.461	38.912
Pit-4a	Pitcairn	-25.072	-130.114	1.0–0.4 Ma	Garapic et al. (2015)	-0.26	0.07	2.82	-0.30	0.04	0.982	0.001	-19	2.03	48.9	4.3	41		40	10	44	0.191	4.15	0.704748	0.512533	17.789	15.492	38.970
Pit-7	Pitcairn	-25.064	-130.117	1.0–0.4 Ma	Garapic et al. (2015)	-0.59	0.07	1.51	-0.32	0.05	0.965	0.001	-36	0.90	48.2	6.4	52		41	8	63	0.212	6.95	0.704824	0.512589	17.833	15.494	38.982
Pit-8	Pitcairn	-25.064	-130.117	1.0–0.4 Ma	Garapic et al. (2015)	-0.34	0.07	1.07	-0.25	0.05	0.978	0.002	-22	0.60	46.3	11.9	65		40	7	60	0.246	7.30	0.704633	0.512538	17.900	15.494	38.976
Pit-12	Pitcairn	-25.065	-130.120	1.0–0.4 Ma	Garapic et al. (2015)	-0.75	0.08	1.28							49.2	6.3	52		42	9	89	0.235	8.37	0.704975	0.512518	17.789	15.487	38.975
Pit-13	Pitcairn	-25.065	-130.120	1.0–0.4 Ma	Garapic et al. (2015)	-0.71	0.07	1.14	-0.21	0.06	0.933	0.001	-67	1.02	47.5	8.1	57		41	9	88	0.255	6.90	0.704999	0.512518	17.735	15.474	38.943
Pit-16	Pitcairn	-25.065	-130.120	1.0–0.4 Ma	Garapic et al. (2015)	-0.34	0.06	2.21	-0.35	0.05	1.021	0.002	21	0.82	48.7	4.5	43		42	10	56	0.203	9.30	0.704687	0.512590	18.131	15.515	38.926
CE-1a	St. Helena	-16.003	-5.721	Miocene	Graham et al (1992); major and trace elements	-0.57	0.06	1.12	-0.31	0.05	1.005	0.001	5	0.72	44.9	13.2	66	0.26	34.2	6	53	0.201	4.66	0.702895		20.890	15.789	40.173
CE-6	St. Helena	-16.01	-5.73	Miocene	Graham et al (1992); major and trace elements	-0.12	0.05	3.22	-0.38	0.04	0.925	0.001	-75	6.55	59.8	1.0	33	2.67	50.2	8	92	0.201	5.44			20.820	15.778	40.106
CE-9*	St. Helena	-16.01	-5.73	Miocene	Graham et al (1992); major and trace elements	-0.42	0.07	1.33							45.7	16.5	70	1.96	34.9	7	40	0.236	3.84			20.685	15.737	39.957
CE-13	St. Helena	-15.99	-5.77	Miocene	Graham et al (1992); major and trace elements	-0.25	0.07	2.10	-0.33	0.04	1.000	0.001	0	1.00	45.8	5.8	44	0.74	39.7	8	34	0.216	4.12	0.702877		20.807	15.796	40.141
CE-14	St. Helena	-15.99	-5.77	Miocene	Graham et al (1992); major and trace elements	-0.84	0.06	1.81	-0.31	0.07	1.018	0.002	18	1.08	49.7	3.9	37	0.67	47.1	12	67	0.220	6.33			20.783	15.771	40.071
CE-18	St. Helena	-15.95	-5.64	Miocene	Graham et al (1992); major and trace elements	-0.71	0.04	1.63	-0.20	0.07	0.978	0.001	-22	0.78	46.9	6.3	47	3.14	38.0	9	62	0.188	8.01	0.702874		20.520	15.735	39.890

Note - δ^{98}Mo values given relative to NIST 3134 (with that standard set to 0). δ^{238}U values given relative to SRM-112a (standard set to 0). CIA is chemical index of alteration from Nesbitt and Young (1982, 1984). W is weathering index from Ohta and Arai (2007). See text for further details.
* - Pb isotope data for CE-9 was obtained by M. Jackson using the P54 MC-ICP-MS at the Department of Terrestrial Magnetism following methods of Jackson et al. (2014) and has not been previously published.

Exploration of Mo isotope systematics of OIBs has been more limited. King et al. (2016) and Gaschnig et al. (2021) reported data for Hawaii and Yang et al. (2015) reported data Iceland, all of which overlapped with MORB. Liang et al. (2017) reported results from Galapagos, Loihi, and several Atlantic OIB localities, with an overall mean δ^{98}Mo of −0.14 ± 0.06 (2σ), overlapping with the MORB range seen by Bezard et al. (2016). Values both heavier and lighter than MORB were reported for some OIB localities in an abstract by Willbold et al. (2012) (also cited in Willbold and Elliott, 2017), but the complete dataset has not been published.

2.2. The U isotope system

Like Mo, U is a redox-sensitive metal most commonly found in either an insoluble 4+ or a soluble 6+ state. The two long-lived isotopes of U (^{235}U and ^{238}U) are also fractionated by some of the same processes as Mo. Scavenging of U(VI) from seawater in oxic depositional environments leads to the preferential enrichment of ^{235}U in sediments and a δ^{238}U (defined as [(^{238}U/^{235}U sample / ^{238}U/^{235}U standard (CRM-112a)) – 1)x1000], where CRM-112a is set to 0‰) lower than seawater (Stirling et al., 2007; Weyer et al., 2008). Unlike Mo, partial reduction of dissolved U(VI) leads to the preferential enrichment of the heavy isotope in sediments deposited in anoxic settings (Stirling et al., 2007; Weyer et al., 2008). An additional source of isotope fractionation is the alteration of basaltic ocean crust by seawater. δ^{238}U values both greater and lesser than unaltered MORB have been reported (Andersen et al., 2015; Noordmann et al., 2015).

Exploration of U isotope variability in igneous systems has been more limited than for Mo. Hiess et al. (2012) analyzed the ^{238}U/^{235}U in a wide range of different U-bearing minerals from different bulk lithologies and used the results to redefine the bulk Earth ^{238}U/^{235}U value from 137.88 to 137.818 (see also Livermore et al., 2018 and Tissot et al., 2019). Telus et al. (2012) analyzed samples of I, S, and A type granites and found only limited variation δ^{238}U and a lack of correlations that might suggest the influence of processes such as fractional crystallization or thermal diffusion; Gaschnig et al. (2021) reported a similar lack of isotopic fractionation with differentiation in the Kilauea Iki lava lake. Andersen et al. (2015) presented U isotope data for MORBs, OIBs, and arc basalts. This landmark study revealed small but systematic differences in δ^{238}U values between the three basalt groups. The heaviest compositions were found in MORBs, with an average δ^{238}U value of −0.268 ± 0.011‰, whereas OIBs gave a slightly lighter average composition of −0.308 ± 0.005‰. Samples from the Mariana arc were isotopically lighter still, with δ^{238}U ranging from −0.419 to −0.323‰. Samples of altered ocean crust and ocean sediments were also sampled. The former were highly variable but generally skewed isotopically heavy, with some positive δ^{238}U, while the latter overlapped with many of the arc basalts. To explain the differences between arc basalts, MORBs, and OIBs, Andersen et al. (2015) constructed a model where altered ocean crust releases some of its U budget into fluids that preferentially remove the light isotope into the arc magma generation region. As the slab travels deeper, fluids from deeper in the ocean crustal section remove isotopically heavy U, leaving the U remaining in the slab with an overall composition like MORB. They argued that this state of affairs has only existed since the oceans became fully oxygenated about 600 million years ago, whereas prior to that, the isotope composition of U was uniform throughout the Earth, with a chondritic δ^{238}U of −0.3‰. The chondritic isotope composition of OIBs was attributed to the antiquity of the OIB source regions, which contain material that was subducted long before the full oxygenation of the oceans. Importantly, most of the OIB samples considered by Andersen et al. (2015) came from North Atlantic hot spots.

A few additional studies have focused on U isotopes in arcs. Avanzinelli et al. (2018) reported δ^{238}U from Vesuvius that were comparable to and heavier than MORB (in contrast to the relatively light values previously reported for the Mariana arc; Andersen et al., 2015), which

they attributed to melting of carbonated subducted sediments. Freymuth et al. (2019) reported results from Izu arc lavas that either overlapped with or extended to lighter compositions than those observed in the adjacent Mariana arc by Andersen et al. (2015). Like Andersen et al. (2015), they argued that fluids preferentially removed the light isotope of U from the slab but suggested that this U was being drawn from the deeper unaltered portion of the subducting ocean crust.

U isotope analyses typically include measurement of ^{234}U, which is an intermediate product in the ^{238}U decay series. It occurs early in the series following the exceedingly short-lived ^{234}Th ($t_{1/2} = 24.1$ days) and ^{234}Pa ($t_{1/2} = 6.7$ h) and has the longest half-life ($t_{1/2} = 246$ kiloyears) of all the intermediate daughters. $^{234}U/^{238}U$ disequilibrium is widely observed in the Earth-surface environment, with dissolved U in many rivers and the oceans showing a ^{234}U excess, which has been attributed to preferential leaching of ^{234}U from alpha recoil-damaged sites during incongruent chemical weathering of crustal rocks (e.g., Thurber, 1962; Sarin et al., 1990; Chabaux et al., 2003). As a result, rocks that have experienced U-loss weathering may develop a ^{234}U deficiency, while rocks that experience U uptake may develop a ^{234}U excess (e.g., Bacon, 1978; MacDougall et al., 1979; Moreira-Nordemann, 1980). If this open system behavior occurs as a transient event more than ~1 million years ago, the $^{234}U/^{238}U$ may return to secular equilibrium.

3. Methods

3.1. Samples

Samples reported here are from Samoa, Pitcairn, and St. Helena, and all have been geochemically characterized in previous studies (see Table 1 and supplemental material). Samoan samples are from multiple islands and submarine volcanoes. AVON3–78-1 is a dredge sample from Malumalu with an age less than 8 ka (Sims et al., 2008). Samples beginning with "ALIA" are dredge samples from Savai'i with an age around 5 Ma (Koppers et al., 2011). The other Samoan samples are subaerial. S16 is from Savai'i and approximately 0.3 Ma (McDougall, 2010). OFU-04-03 and T33 are from Ofu and Ta'u, respectively, and are less than 0.3 Ma (McDougall, 2010). Major and trace element and radiogenic isotope data for the Samoan lavas is available for these samples in Workman et al. (2004), Jackson et al. (2007a, 2007b), and Hart and Jackson (2014). The samples from Pitcairn were reported on in Garapić et al. (2015) and range from 0.4 to 1.0 Ma. The samples from St. Helena were reported on by Graham et al. (1992) and range from 7 to 15 Ma. New major element and trace element for the St. Helena samples were obtained by XRF and ICP-MS from the Geoanalytical Laboratory at Washington State University following the methods of Johnson et al. (1999) and Knaack et al. (1994) (see supplemental file). A new Pb isotope analysis was obtained for St. Helena lava CE-9 using the P54 MC-ICP-MS housed at the Department of Terrestrial Magnetism, following the methods of Jackson et al. (2014)). All samples from all localities are mafic except for ALIA-115-21 from Samoa and CE-6 from St. Helena, which are trachyandesite and phonolite, respectively.

3.2. Digestion

Samples were digested for Mo and U isotope analysis at the Georgia Institute of Technology with approximately 0.1 g of powder combined with 4 mL of concentrated trace metal-grade HF plus 0.5 mL of concentrated once distilled HNO_3 at 140 °C in acid-cleaned, screw-top Teflon beakers on a hot plate. Beakers were uncapped and acids were evaporated. Salts were dissolved in 4 mL of concentrated HNO_3 and

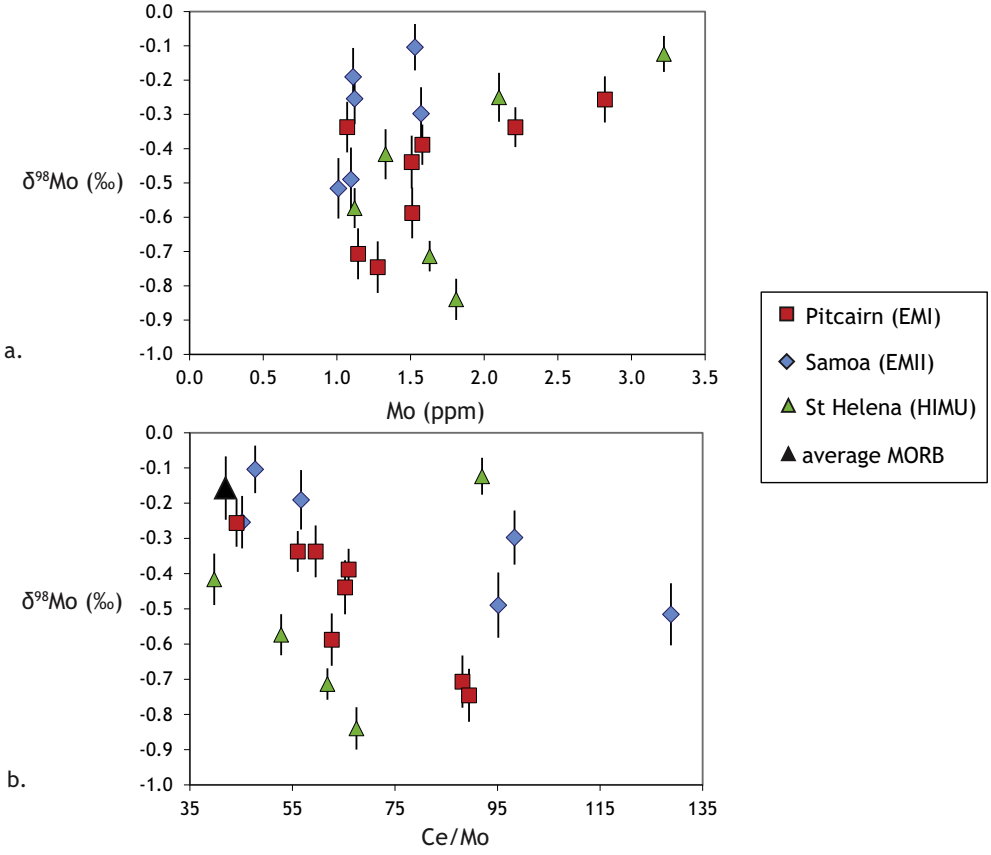

Fig. 1. $\delta^{98}Mo$ vs. (a) Mo concentration and (b) Ce/Mo. $\delta^{98}Mo$ here and elsewhere is given relative to NIST-3134 (i.e., NIST-3134 = 0‰). While there is generally little correlation between $\delta^{98}Mo$ and [Mo], $\delta^{98}Mo$ and Ce/Mo are generally well correlated in a negative sense. Samples from the three localities form arrays that radiate away from average MORB (composition from Bezard et al., 2016). Error bars for Mo isotope compositions here and elsewhere are 2 standard error level.

evaporated and then repeatedly dissolved in once-distilled 6 M HCl and evaporated until a solution free of precipitates was obtained.

3.3. Mo separation and isotope ratio analysis

Sample solutions were mixed with a ^{97}Mo—^{100}Mo double spike in proportions designed to double Mo concentration in the resulting mixture and then dried down. Mo chromatography was performed at Georgia Institute of Technology using the single stage "procedure 2" of Willbold et al. (2016), which was designed specifically for igneous rocks and typically removes the sample matrix in one pass.

Purified Mo solutions were analyzed for isotope composition at the Yale Metal Geochemistry Center on a Thermo Neptune Plus MC-ICP-MS. Solutions were introduced with an Apex IR desolvating nebulizer and analyzed in static mode. ^{91}Zr and ^{99}Ru were monitored to correct for potential isobaric interference. Groups of three samples were bracketed with analyzes of the spiked NIST 3134 Mo isotope standard and by periodic analyses of the spiked RochMo2 Mo standard. Mo isotope compositions are reported in δ^{98}Mo relative to NIST 3134 (i.e., with NIST 3134 set to 0‰) (Goldberg et al., 2013). While Nägler et al. (2014) recommended defining the δ^{98}Mo of NIST 3134 as +0.25‰, in order to allow for easy comparison to published seawater and sediment data that

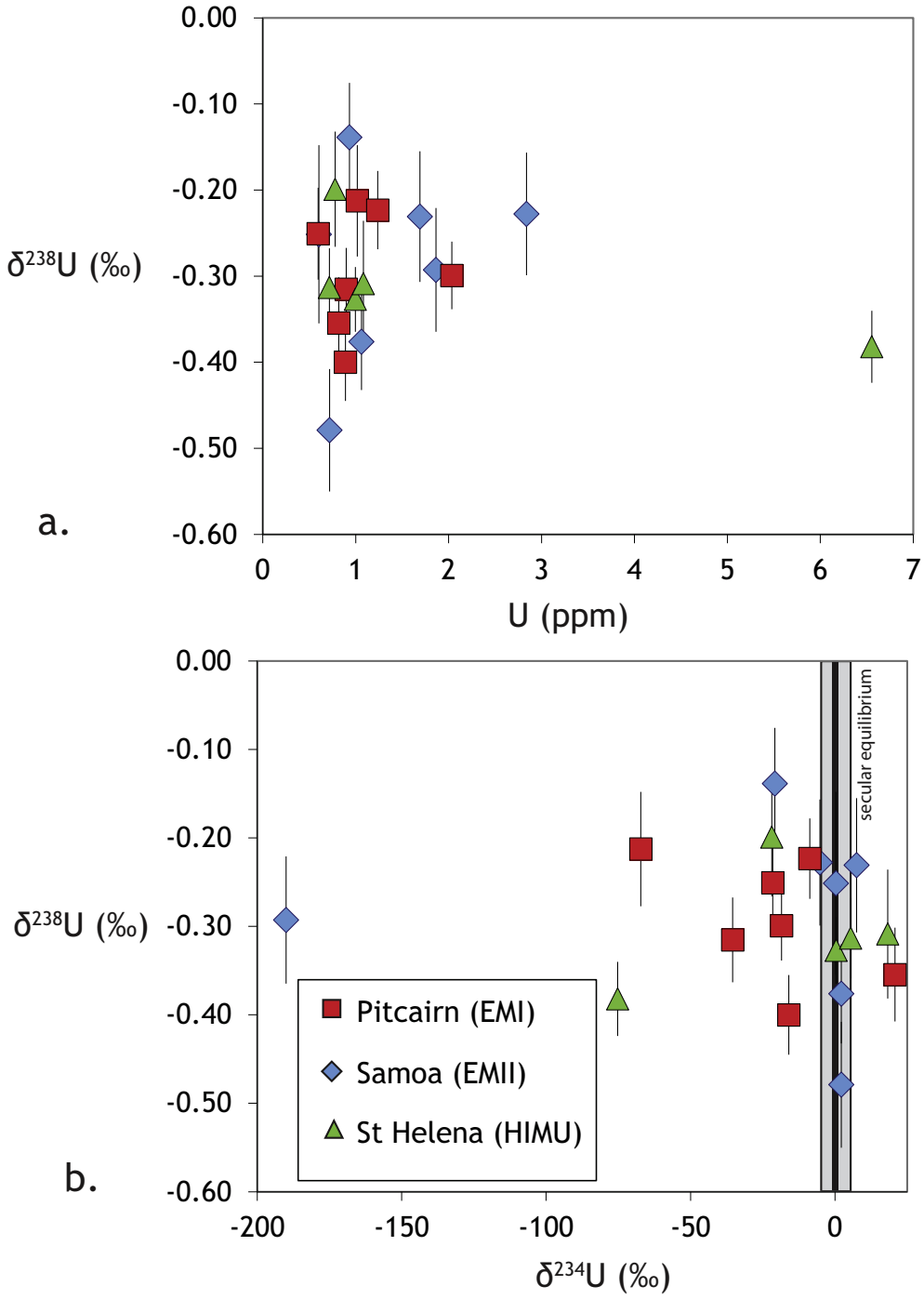

Fig. 2. δ^{238}U vs (a) U concentration and (b) δ^{234}U. There are not apparent correlations between δ^{238}U and either parameter. Importantly, many samples are not at secular equilibrium with regards to δ^{234}U, defined as within ±7‰ of 0‰ (shown by the gray shaded band here and in subsequent figures). Error bars for U isotope compositions here and elsewhere are 2 standard error level.

were normalized to different standards, the majority of studies of Mo isotopes in igneous rocks have reported results relative to NIST 3134 with that standard set to 0‰.

External reproducibility on NIST 3134 was ±0.04‰. Most of the samples reported in this study were analyzed in the same batches as those in Gaschnig et al. (2017). This includes aliquots of the USGS reference materials BHVO-2 and W-2. δ^{98}Mo values of −0.08 ± 0.03‰ (2σ, $n = 4$) for BHVO-2 and -0.04 ± 0.08‰ (2SE, $n = 1$) for W-2 were reported in that earlier study, which are consistent with published values (Burkhardt et al., 2014; Hin et al., 2013; Li et al., 2014; König et al., 2016; Bezard et al., 2016; Zhao et al., 2016). We note that while BHVO-2 is a Hawaiian basalt and therefore an OIB, the effects of metal contamination during the preparation of this and other USGS basalt standards (Weis et al., 2005, 2006; Willbold et al., 2016) make them unreliable as sources of additional data on Mo isotope heterogeneity in the mantle. Final analyses for this study included USGS reference materials SDO-1 and NOD-A. δ^{98}Mo values obtained for these 0.76 ± 0.10‰ (2σ, $n = 2$,) and − 0.69 ± 0.08‰ (2SE, n = 1), both of which are consistent with published values (Goldberg et al., 2013; Li, and Zhu, X.-k., Tang, S.-h., Zhang, K., 2016; Zhao et al., 2016). Quoted uncertainties in Table 1 and error bars in figures are internal two standard errors, as these uncertainties are generally greater than the reproducibility on NIST 3134.

3.4. U separation and isotope ratio analysis

Sample solutions were mixed with a ^{233}U—^{236}U double spike in amounts appropriate to yield a ^{238}U/^{236}U of 30 in the resulting mixtures. Samples were dried down and brought up in 3 M HNO_3 for column chromatography. U was purified in one pass with UTEVA resin, following the methods of Wang et al. (2016) (modified from Weyer et al., 2008). Isotope analyses were conducted at the Yale Metal Geochemistry Center on a Thermo Neptune Plus MC-ICP-MS. Samples were normalized to bracketing analyses of spiked CRM 112a solutions. Additional details are provided in Wang et al. (2016). The long-term reproducibility of the δ^{238}U and δ^{234}U compositions of CRM 112a are ±0.07‰ and 4‰, respectively. Four analyses of the USGS BHVO-2 reference material were also analyzed and yielded a δ^{238}U of −0.34 ± 0.05‰ and δ^{234}U of 4 +/− 4‰, overlapping with published values (Andersen et al., 2015; Tissot and Dauphas, 2015). Quoted uncertainties in Table 1 and error bars in the figures are internal two standard errors, which generally are comparable to the reproducibility of CRM 112a.

4. Results

4.1. Mo isotope results

δ^{98}Mo results for each locality are highly variable and significant

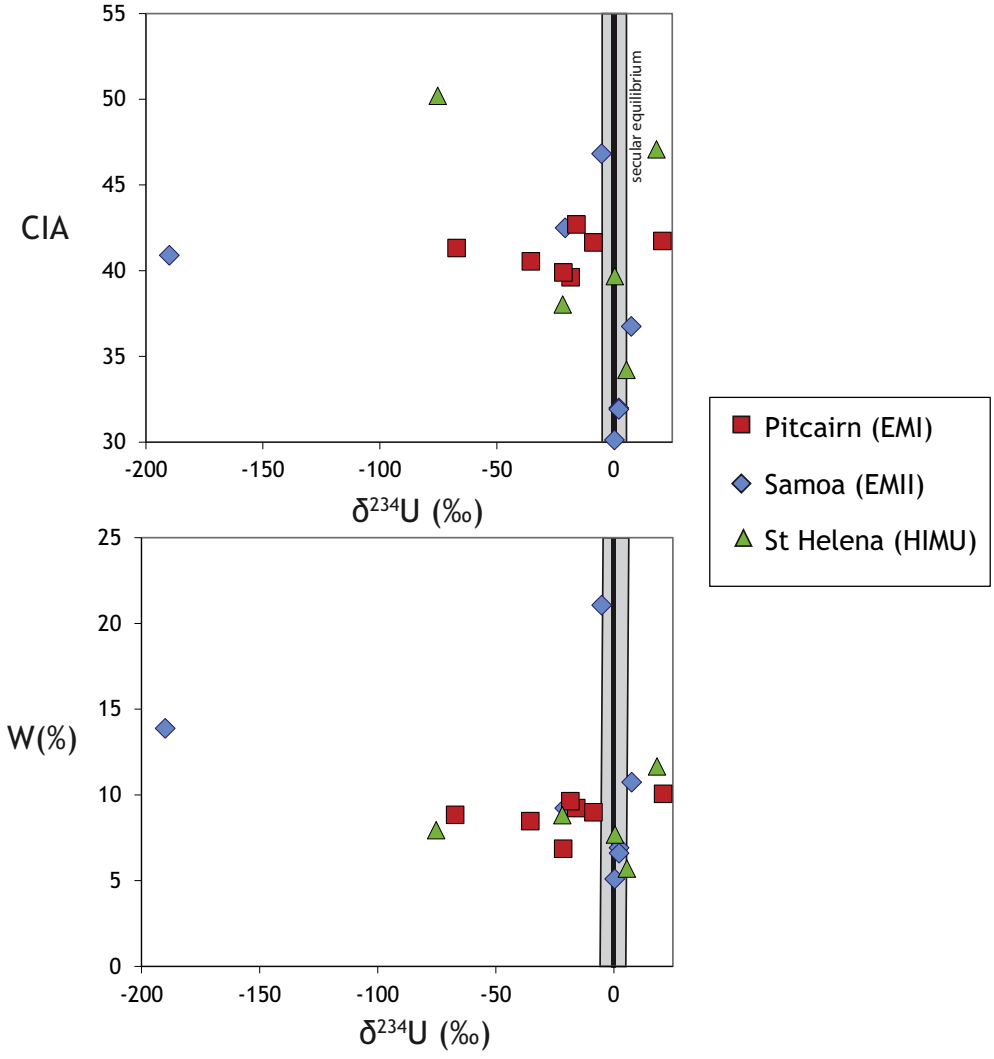

Fig. 3. δ^{234}U vs the (a) CIA and (b) W, two different major-element based indices for chemical weathering and alteration (see text). Samples with δ^{234}U disequilibrium tend to have higher CIA and slightly higher W values. Major element sources given in text.

overlap exists between the ranges of compositions seen amongst the three localities (Fig. 1). Samoa samples have δ^{98}Mo values ranging from −0.10‰ to −0.52‰, Pitcairn samples have −0.26‰ to −0.75‰, and St. Helena samples have δ^{98}Mo values from −0.12‰ to −0.84‰. Mo concentrations show significant overlap amongst localities and range from 1.0 to 3.2 ppm. While correlations between [Mo] and δ^{98}Mo are not particularly strong, the samples from Pitcairn and St. Helena with the highest Mo content also have the highest δ^{98}Mo values. All samples have Mo isotope compositions significantly lighter than the continental crust (which typically has positive δ^{98}Mo values) (Yang et al., 2017), and most are lighter than the range seen in MORBs (Bezard et al., 2016). The δ^{98}Mo variability is significantly reduced after samples exhibiting evidence of low temperature alteration are excluded (see Discussion).

4.2. U isotope results

As with the Mo isotope data, δ^{238}U results from the individual localities show heterogeneity, and there is significant overlap in the ranges seen between the localities (Fig. 2). Samoa samples have δ^{238}U values ranging from −0.23‰ to −0.48‰, Pitcairn samples have values ranging from −0.21‰ to −0.40‰, and St. Helena samples have values ranging from −0.21‰ to −0.38‰. δ^{238}U values from each locality overlap with values reported for both MORB and other OIB localities by Andersen et al. (2015). U concentrations vary from 0.6 to 2.8 ppm for Samoa and

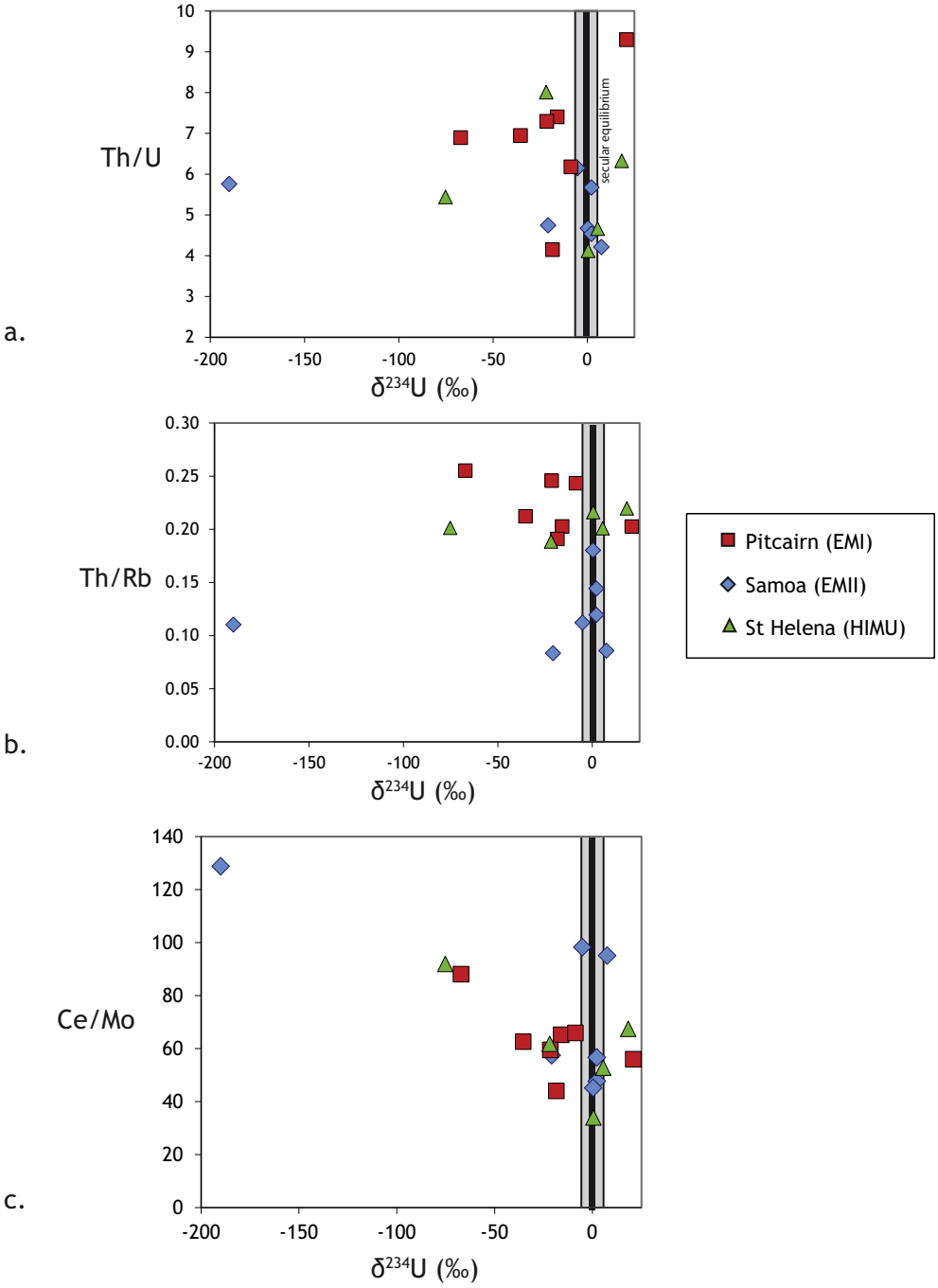

Fig. 4. δ^{234}U vs trace element ratios. Chemical weathering would be expected to preferentially remove (a) U and (b) Rb over Th but there is not a strong correlation with δ^{234}U. On the other hand, Ce/Mo (c) shows a relatively clear inverse relationship with δ^{234}U for each location, suggesting that Mo was mobilized by the same process that disturbed the ^{234}U/^{238}U. Trace element sources given in text.

0.6 to 2.3 ppm for Pitcairn. The phonolite sample from St. Helena has high [U] of 6.55 ppm, but the other samples from that locality range from 0.7 to 1.1 ppm.

Importantly, U isotope analysis provides $^{234}U/^{238}U$ ratios in addition the $^{238}U/^{235}U$. Samples at secular equilibrium will have $^{234}U/^{238}U$ activity ratios equal to 1 and $\delta^{234}U$ values within uncertainty of 0‰. Values deviating from secular equilibrium suggest the lavas behaved as open systems with regard to U after crystallization and within the last ~1 Ma. The majority of samples studied here have $\delta^{234}U$ values indicating secular disequilibrium (Fig. 2b), where secular equilibrium is defined here by $\delta^{234}U$ values deviating more than ±7‰ from 0‰. Of these, most show a deficit in ^{234}U. The most extreme value in the whole dataset is −190‰ in a Samoan sample; the other Samoan samples range from −21‰ to +7‰, with three at secular equilibrium. (Of the three in equilibrium, $^{234}U/^{238}U$ results were previously reported for sample AVON3–78-1 by Sims et al., 2008 and are within uncertainty of our results). Samples from Pitcairn range from −67‰ to +21‰, and none are at secular equilibrium. Samples from St. Helena range from −75 to +18‰, with two at secular equilibrium. We note that U isotope data is unavailable for one Pitcairn and one St. Helena sample that were analyzed for Mo isotopes.

5. Discussion

5.1. Interpretation and significance of uranium secular disequilibrium

The ^{234}U deficiency seen in many of the samples studied here point to some degree of U loss presumably during chemical weathering while the few samples with a ^{234}U excess presumably gained U through interaction with either seawater (directly or perhaps via sea spray) or surface runoff. Many of the samples studied here are older than 1 Ma, and if alteration and disturbance of $^{234}U/^{238}U$ occurs as a transient event before 1 Ma, the system will revert to secular equilibrium and the alteration event will be masked. However, the presence of $^{234}U/^{238}U$ disequilibrium in the samples studied is not confined to only <1 Ma samples. Three Miocene samples from St. Helena and one from Samoa show disequilibrium. This is not surprising as chemical weathering tends to operate as a slow but continuous process. Furthermore, in these relatively simple volcanic island settings, a scenario of early chemical weathering followed by stasis (allowing $^{234}U/^{238}U$ to revert to equilibrium) seems less likely than early burial by subsequent lava flows followed by more recent erosion and exposure to chemical weathering, yielding still measurable $^{234}U/^{238}U$ disequilibrium.

Indicators of chemical alteration come from numerous indices based on major element compositions. The most notable one is the chemical index of alteration (CIA), defined as Al_2O_3 / (Al_2O_3 + CaO* + Na_2O + K_2O) with oxides given in molar portions and CaO* corrected for any calcium-bearing carbonate or phosphate and higher values being consistent with greater weathering or alteration (Nesbitt and Young, 1982, 1984). Fig. 3a shows $\delta^{234}U$ versus CIA values, and these parameters are not well-correlated, although the samples at secular equilibrium do have the lowest CIA values. However, a weakness of the CIA is that different unweathered lithologies have different starting values, with basalts significantly lower (e.g., ~40) than granites (~low to mid

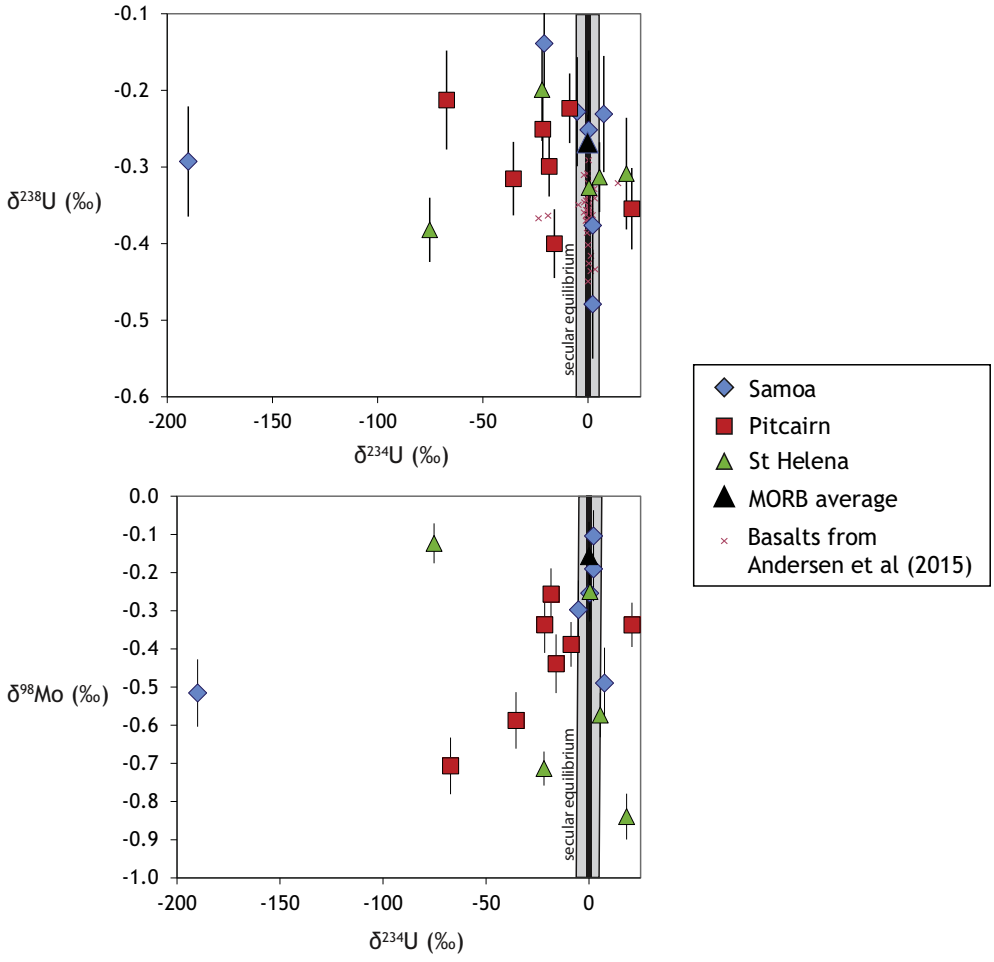

Fig. 5. $\delta^{234}U$ vs (a) $\delta^{238}U$ and (b) $\delta^{98}Mo$. While there is not a clear correlation between $\delta^{234}U$ and $\delta^{238}U$, most of the samples with lower $\delta^{98}Mo$ values show evidence of U-loss. Small red x's in (a) are data from Andersen et al. (2015).

50s). Ohta and Arai (2007) used principal component analysis of a large database of different fresh igneous lithologies and sediments to develop an alternate weathering index meant to deconvolve the source rock composition of weathering effects. This system provides fractions of F, M, and W (for felsic, mafic, and weathered) for given major element compositions. In Fig. 3b, $\delta^{234}U$ is compared to W; as with the CIA, samples at secular equilibrium tend to have the lowest W values, although the parameters are otherwise not well correlated.

Trace element ratios may also provide additional evidence of weathering or alteration effects. Thorium and uranium have very similar behavior in igneous systems, but Th remains insoluble and immobile during weathering while U may be oxidized from +4 to its soluble +6 state. The Th/U should therefore increase during chemical weathering and might be expected to correlate with $\delta^{234}U$. While the lavas of Pitcairn are notable in having unusually high primary Th/U ratios that appear to be unique to that plume source (Eisele et al., 2002), internal correlations between Th/U and $\delta^{234}U$ for this and the other localities might still be expected. These parameters are shown in Fig. 4a and no clear correlation is present, although the St. Helena samples in $^{234}U/^{238}U$ disequilibrium tend to have higher Th/U. Other elements prone to open-system behavior during chemical weathering include alkalis such as Rb; leaching should remove (or submarine alteration should add) Rb relative to insoluble elements such as Th. However, fig. 4b shows a lack correlation between Th/Rb.

Conversely, a stronger relationship is present between Ce/Mo and $\delta^{234}U$ (Fig. 4c), with disequilibrium samples generally exhibiting increasingly elevated Ce/Mo values. The Ce/Mo ratio is frequently used in studies of the Mo isotope tracer in igneous systems (e.g., Freymuth et al., 2015) because Mo is thought to show similar compatibility to Ce during mantle melting (Ce/Mo = 32 in MORB; Newsom and Palme, 1984; Newsom et al., 1986). Variations in Ce/Mo in arc basalts have been attributed to fractionation of these two elements during slab devolatilization, with Mo more easily transferred to the mantle wedge by fluids, leaving slab residues entering potential OIB source regions with a higher Ce/Mo (e.g., Freymuth et al., 2015; Skora et al., 2017). This may explain the high Ce/Mo values seen in some Samoan samples with $^{234}U/^{238}U$ at equilibrium. However, Mo is quite soluble during weathering under oxidizing conditions, especially compared to rare earth elements (e.g., Kendall et al., 2017). Furthermore, studies of Mo mineral residency in basalts have shown that it tends to be concentrated in easily weatherable glass (Greaney et al., 2017). King and Pett-Ridge (2018) found that the loss of Mo during chemical weathering of basalt was particularly high during its incipient stage. Consequently, the strong negative relationship between Ce/Mo and $\delta^{234}U$ and the more muted relationships between $\delta^{234}U$ and other tracers suggests that Mo is lost more quickly and readily.

It is important to consider whether incipient weathering is accompanied by $^{238}U/^{235}U$ and $^{98}Mo/^{95}Mo$ fractionation. Studies of $^{238}U/^{235}U$ as a possible petrogenetic tracer have typically used ^{234}U disequilibrium in samples as a criterion for rejection of the associated $^{238}U/^{235}U$ under the assumption that the latter is compromised during U-loss or U-gain from a sample. While we are not aware of any systematic study of $\delta^{238}U$ behavior in weathering profiles, the similarity between the $\delta^{238}U$ in river water to the average continental crust suggests that chemical weathering does not significantly fractionate ^{238}U from ^{235}U (Andersen et al., 2016). Fig. 5a shows $\delta^{234}U$ versus $\delta^{238}U$, and no apparent relationship between these parameters is present. Many of the samples with $^{234}U/^{238}U$ disequilibrium have $\delta^{238}U$ that overlap with the average composition of MORB (Andersen et al., 2015), and the sample with the most negative $\delta^{238}U$ is in $^{234}U/^{238}U$ equilibrium. Conversely, nearly all samples with either ^{234}U excess or deficiency have isotopically light Mo, and the Samoa and Pitcairn samples with the greatest ^{234}U deficit also have the lightest Mo isotope signature. Given the already discussed Ce/Mo-$\delta^{234}U$ and Ce/Mo- $\delta^{98}Mo$ relationship, this strongly suggests that Mo was leached during chemical weathering and that the heavy isotopes of Mo were preferentially lost during this chemical weathering. Preferential loss of isotopically heavy Mo during weathering was first suggested when it was recognized that rivers tend to contain dissolved Mo loads with isotopic compositions generally heavier than the bulk crust (Archer and Vance, 2008; Pearce et al., 2010; Voegelin et al., 2012; King and Pett-Ridge, 2018; Horan et al., 2020). Leaching experiments likewise found that leachates tend to have isotopically heavier Mo than residue (Liermann et al., 2011; Voegelin et al., 2012), and studies of weathering profiles of basalt have noted that lower saprolitic portions of the profiles tend to have isotopically light Mo relative to unweathered source rock (Greaney et al., 2021; Liu et al., 2020; Wang et al., 2020).

To summarize, evidence presented here suggests that samples with $^{234}U/^{238}U$ disequilibrium may also have disturbed Mo isotope compositions. These samples should not be considered further in terms of interpretations of the Mo isotope compositions of the plume sources. It is less clear if the $\delta^{238}U$ values here have been affected, but the most conservative approach is to discount these results in the subsequent discussion. Finally, these results highlight the unique utility of the $^{234}U/^{238}U$ ratio in detecting cryptic or incipient alteration that might not be detected by other chemical tracers or indices.

5.2. General implications for mantle sources

Here, we consider the implications for OIB sources derived from the Mo and U compositions of the samples with $^{234}U/^{238}U$ equilibrium

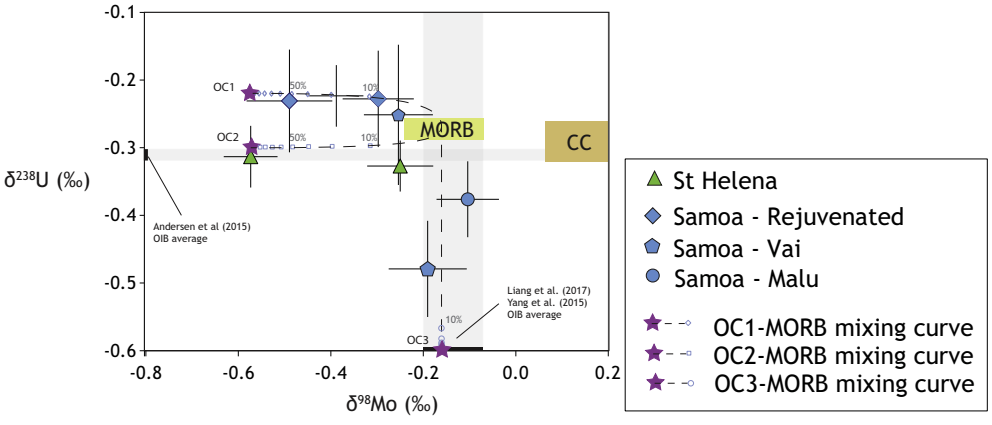

Fig. 6. $\delta^{238}U$ vs. $\delta^{98}Mo$ results for only samples with ^{234}U—^{238}U equilibrium. Note that all Pitcairn samples analyzed for U isotopes show ^{234}U—^{238}U disequilibrium and are therefore not shown. The average composition for MORB is from Bezard et al. (2016) and Andersen et al. (2015), the average composition of the continental crust (orange rectangle) (based on data derived from granites) is from Yang et al. (2017) and Tissot and Dauphas (2015), and the average $\delta^{98}Mo$ and $\delta^{238}U$ values of other analyzed OIB localities is from Yang et al. (2015), Liang et al. (2017), and Andersen et al. (2015). Published OIB data shows a narrow range that is close to that of MORB, perhaps because many of the sampled localities are ridge-intersecting hot spots. Mixing pathways between MORB and subducted ocean crust using Mo isotope data from Chen et al. (2019) and hypothetical U isotope values are shown. End member compositions are given in supplementary table.

compositions (i.e., samples with $\delta^{234}U = 0 \pm 7‰$) (Fig. 6). The St. Helena samples are skewed towards lighter-than-MORB Mo isotope compositions, and U isotope compositions are within uncertainty of or slightly lighter than MORB. Samples from Samoa are divided between those with similarly light Mo isotope compositions but MORB-like U isotope compositions and those with anomalously light U isotope composition and MORB-like Mo isotope compositions. As discussed above, light Mo isotope compositions are most associated with sediments deposited under oxic conditions, especially those rich in Fe—Mn oxides/hydroxides. Addition of such material to plume sources would therefore seem to provide the most straightforward explanation for the isotopically light compositions seen in the localities. Such materials also would be expected to have U isotope compositions lighter than MORB (albeit with a smaller isotopic shift due to the smaller range of isotope fractionation observed in nature for U). However, sedimentary addition places time constraints on the age of subducted material incorporated into the plume source regions, as it requires those subducted sediments to have been deposited under a fully oxidized ocean, and such conditions did not become the norm until at least the Neoproterozoic. Sediments deposited in the earlier Proterozoic and especially the Archean are likely to contain Mo and U with isotope compositions broadly similar to the continental crust (i.e., heavier than MORB for Mo; Kendall et al., 2017 and references therein).

An additional complication with the scenario outlined above is that there is a potential for the isotope fractionation of Mo in the subducting slab package (i.e., ocean lithosphere plus sediment cover) during slab

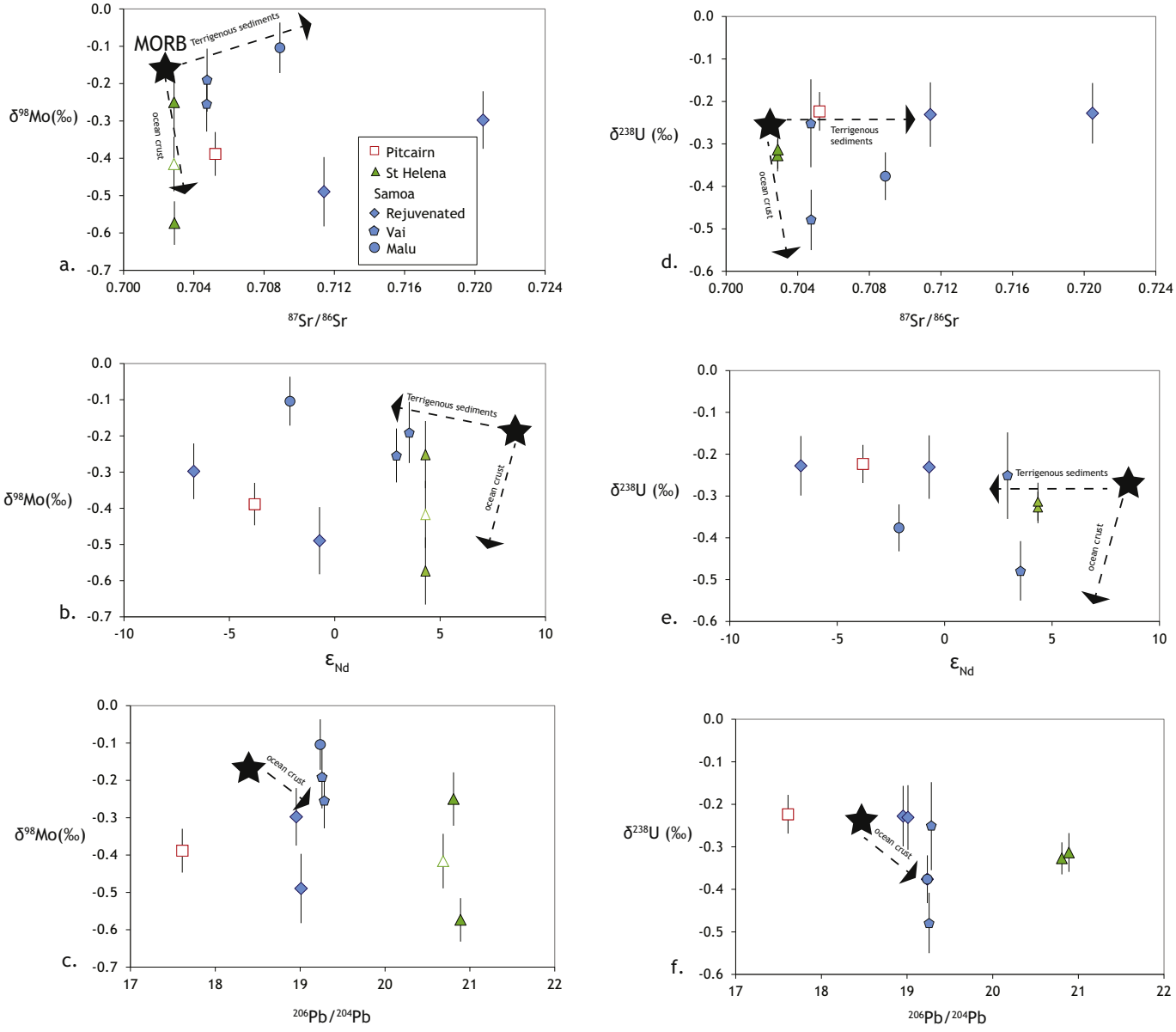

Fig. 7. Mo and U isotope signatures vs published Sr, Nd, and Pb isotope data for the same samples. Samples with $^{234}U—^{238}U$ disequilibrium are not shown; one sample St. Helena and one from Pitcairn with Mo isotope data but no U isotope data are shown as open symbols in (a) through (c)since the $^{234}U—^{238}U$ disequilibrium filter cannot be applied. No Nd isotope results are available for these St. Helena samples and Sr results are only available for some; however, the Sr and Nd isotope range observed at St. Helena is exceedingly narrow so mean values from Hanyu et al. (2014) were assigned to these samples. Schematic arrows indicate the trajectories expected for the incorporation of either subducted terrigenous sediment or ocean crust into a MORB-like mantle source. Most of the variation in the results can attributed to mixing of these three components. Note that for $^{206}Pb/^{204}Pb$ isotope compositions of subducted sediment will vary greatly based on age and the extent to which U and Pb are decoupled by subduction metamorphism, meaning that their contribution to a MORB-like mantle could either increase or decrease the resulting ratio so no trajectory for this scenario is given in (c) and (f).

dehydration so that material incorporated into the plume source regions would not necessarily preserve the same isotope signatures it acquired at the surface. As previously mentioned, several studies of Mo isotopes in arc systems have concluded that Mo must be isotopically fractionated during dewatering of ocean crust, leaving behind residual material with an isotopically light signature that pollutes the OIB source regions (Casalini et al., 2019; Freymuth et al., 2015; König et al., 2016; Skora et al., 2017; Willbold and Elliott, 2017). The relationship between d^{98}Mo and Mo/Ce in the OIBs reported on by Liang et al. (2017) also supports this. Further support for isotope fractionation during dewatering was recently provided by Chen et al. (2019), who reported low δ^{98}Mo values in eclogites and blueschists (i.e., rocks which experienced subduction metamorphism and devolatilization).

Fractionation during dewatering has also been invoked for the U isotope system by Andersen et al. (2015) and Freymuth et al. (2019); in this case, fluids preferentially remove the light isotope of U, leading to lower δ^{238}U values in arcs, and the residual crustal material subducted into the deep mantle and OIB source regions may be left with higher δ^{238}U. (This hypothesis has not yet been ground-truthed in high pressure metamorphic rocks as has been done for Mo by Chen et al., 2019). While sampling to date has found significant U isotope heterogeneity in altered ocean crust with δ^{238}U values both higher and lower than unaltered MORB (Andersen et al., 2015; Noordmann et al., 2015), altered ocean crust appears to have a heavier isotope composition than MORB *on average* (Andersen et al., 2015), and the limited loss of isotopically light U during devolatilization will only lead to a further increase in δ^{238}U in the residual ocean crustal material that may be added to the plume source regions. This suggests that OIBs that sample recycled crust should have higher δ^{238}U than MORB, which is the opposite of what is observed. Andersen et al. (2015) explained this by invoking additional episodes of slab devolatilization beyond the arc front that might release heavy U into the convecting upper mantle.

Incorporation of devolatilized subducted ocean crust likely explains the fractionated Mo and U isotope compositions observed here, as the apparent antiquity of the OIB sources (Chauvel et al., 1992; Jackson et al., 2007a, 2007b; Kimura et al., 2016; Andersen et al., 2015; Cabral et al., 2013; Delavault et al., 2015, 2016) would seem to argue against subducted sediments being a principal source, particularly in the case of St. Helena, where published Sr and Nd isotope compositions are either comparable to or only slightly geochemically enriched relative to MORB. Two models of the addition of subducted oceanic crust using the eclogite Mo data from Chen et al. (2019), to an ambient mantle with a MORB-like isotope composition are shown in Fig. 6 (see supplemental table for end members). Both end members (OC1 and OC2) use eclogite sample (SEC-46-1) as an endmember for Mo isotope composition of subducted ocean crust, as this occurs roughly in the middle of the range of Mo isotope compositions reported by Chen et al. (2019). However, the greater uncertainty in the behavior of the U isotope system in the slab, as outlined above, makes the choice of an end member δ^{238}U composition rather arbitrary. OC1 uses a δ^{238}U slightly higher than MORB to explain one of the two groups of Samoan data whereas OC2 is assigned a δ^{238}U that is essentially identical to the bulk Earth (−0.3‰), as defined by meteorites, Atlantic OIBs, and Hawaiian basalt (Andersen et al., 2015). In these models, the lightest observed Mo isotope in the Samoan dataset can be produced with 40% recycled ocean crust added to the MORB reservoir. With the end member chosen here for oceanic crust, the most extreme St. Helena sample would consist entirely of recycled ocean crust, but given the speculative nature of this exercise and the possible range of end member compositions, this is less concerning: for example, use of a different sample from Chen et al. (2019) with a lighter Mo isotope composition would reduce the required fraction of recycled ocean crust and future work on Mo isotopes in high pressure-low temperature metamorphic rocks will undoubtedly expand range of Mo isotope compositions observed in such settings. In any case, ancient ocean crust has been considered a key component in both the Pitcairn and St. Helena sources based on other isotope tracers and trace elements (e.g., Kawabata et al., 2011; Hanyu et al., 2014; Garapić et al., 2015; Blusztajn et al., 2018; Delavault et al., 2015). Validity of the δ^{238}U values chosen for end members can only be assessed through further research on the U isotope, especially in previously subducted high pressure-low temperature metamorphic rocks.

The Mo—U isotope results for Samoa are distinct in that they form two groups, one comparable to St. Helena (low δ^{98}Mo, MORB-like δ^{238}U) and another with MORB-like δ^{98}Mo and unusually low δ^{238}U, and these differences are partially linked to geographic location. Jackson et al. (2014) reported that samples from different island and seamount groups along the Samoan chain have distinct radiogenic isotope trends. Samples of the Vai lineament have dilute HIMU signatures, while samples from the Malu lineament have classic EM-2 signatures, and rejuvenated samples have EM-1-like signatures. Of the three lowest δ^{98}Mo Samoan samples studied here, two are from the rejuvenated trend and one is from the Vai trend. Of the two low δ^{238}U samples, one is from the Vai trend and the other is from the Malu trend.

A low δ^{238}U signature that is seemingly decoupled from δ^{98}Mo, as seen for two of the Samoan samples, may be related to a key difference in the oceanographic behavior of these two isotope tracers. In contrast to Mo, non-quantitative reduction of dissolved U in euxinic depositional environments causes substantial enrichment in the *heavy* isotope of U in associated sediments, which in turn shifts the composition of *all* remaining oceanic sinks of U towards a lighter isotope composition (e.g., Andersen et al., 2017). This effect is at work today (in that deposition of heavy U in the Black Sea drives the remaining oceanic U budget to a lighter isotope composition), but during periods of much greater anoxia or low oxygen conditions, the negative shift in δ^{238}U would be greater in the other sinks (e.g., Montoya-Pino et al., 2010; Andersen et al., 2017). Such conditions appear to have been prevalent between the Paleoproterozoic Great Oxidation Event and the Neoproterozoic Oxidation Event; on the one hand, dissolved oxygen levels were higher than the Archean but euxinic conditions remained more widespread than what would be typical of the Phanerozoic (e.g., Planavsky et al., 2014). In particular, Gilleaudeau et al. (2019) recently reported isotopically light U in carbonates (representing the ocean water composition of the time) ranging from 1.8 and 0.8 Ga in age whereas the oceanic Mo isotope record recorded by black shales during this interval show more muted deviations from crustal values (e.g., Kendall et al., 2011; Asael et al., 2013; Partin et al., 2015). This latter point is important because it argues against a significant pool of sediment with isotopically light Mo being produced and subsequently subducted during the Proterozoic. With this in mind, a distinct Proterozoic pool of subducted material (ocean crust plus sediment) may explain the anomalous U isotope results for Vai and Malu Samoan samples. This is modeled as OC3 in Fig. 6, which has a MORB-like Mo isotope composition but anomalously light U isotope composition. Again, the validity of the model U isotope compositions used here will depend on future work on this isotope system.

Further considerations for the origin of the fractionated Mo and U signatures are provided by comparing those isotope ratios to published Sr, Nd, and Pb isotope data for the same samples (Fig. 7). (Note that one sample from St. Helena and one from Pitcairn have lighter-than-MORB Mo isotope compositions but no U isotope data with which to evaluate alteration effects; these are shown as unfilled symbols in Fig. 7a through 7c for the sake of completeness). Correlations between Mo and U isotopes and the radiogenic isotopes are not strong but much of the covariation can be explained by the mixing a MORB-like reservoir with variable amounts of recycled ocean crust and continentally derived sediment. Mixing of the MORB source with recycled ocean crust alone would likely lead to low δ^{98}Mo and possibly low δ^{238}U, a slight increase and decrease in $^{87}Sr/^{86}Sr$ and ε_{Nd}, respectively, and a potentially large increase in $^{206}Pb/^{204}Pb$ (although age and parent-daughter decoupling during subduction exert a large control). On the other hand, addition of terrigenous sediment will cause a more substantial increase and decrease in $^{87}Sr/^{86}Sr$ and ε_{Nd}, respectively, and probably increase δ^{98}Mo without substantially changing δ^{238}U. Importantly, Neoproterozoic and

younger sediments may develop lighter Mo and U isotope signatures by scavenging the element from seawater (and the effect of euxinia in the earlier Proterozoic as discussed above may also lead to a lighter U isotope signature). While we consider recycled ocean crust to be the major source of fractionated Mo and U isotope signatures, the elevated $^{87}Sr/^{86}Sr$ and lower ε_{Nd} compositions seen in some of the Samoan samples (and Pitcairn) are surely a signpost of subducted sediment.

6. Conclusions

Characterization of the Mo and U isotope compositions of the EM-1, EM-2, and HIMU mantle end members was attempted via analysis of selected OIB samples from Pitcairn, Samoa, and St. Helena. Large-scale variations in both Mo and U were observed with significant overlap across the three localities. Some of this variation is attributable to recent chemical weathering or alteration of the samples, which is revealed by $^{234}U/^{238}U$ disequilibrium in roughly half of the samples, including all of those from Pitcairn that were analyzed for U isotopes. Of these samples, most show a ^{234}U deficit consistent with U loss and samples with greater disequilibrium tend to have more extreme $\delta^{98}Mo$ compositions and higher Ce/Mo, implying that the Mo isotope system was similarly disturbed by alteration. The lack of strong correlation with traditional major and trace element indicators of alteration highlights the unique power of the $^{234}U/^{238}U$ ratio in detecting cryptic or incipient alteration.

Samples with $^{234}U/^{238}U$ in secular equilibrium have $\delta^{98}Mo$ values ranging from comparable to MORB to significantly lower, and the same is true of $\delta^{238}U$. We attribute the low $\delta^{98}Mo$ values and more muted fractionation of U in the St. Helena and some of the Samoa samples to incorporation of ancient devolatilized subducted oceanic crust, which is in line with radiogenic isotope studies. Greater variation is seen in the samples from Samoa, some of which have unusually low $\delta^{238}U$ values but MORB like $\delta^{98}Mo$ values. We speculate that the low $\delta^{238}U$ signature reflects the influence of a distinct pool of subducted oceanic crust dating to the period between the Great Oxidation Event (2.3 Ga) and Neoproterozoic Oxidation Event (0.6 Ga).

Declaration of Competing Interest

The authors declare that they have no known competing financial interests or personal relationships that could have appeared to influence the work reported in this paper.

Acknowledgements

CTR and NJP acknowledge funding from the NASA Astrobiology Institute. This paper was improved by thoughtful reviews from Tim Elliot, Vincent Salters, and an anonymous reviewer.

Appendix A. Supplementary data

Supplementary data to this article can be found online at https://doi.org/10.1016/j.chemgeo.2021.120416.

References

Allègre, C.J., Brévart, O., Dupré, B., Minster, J.-F., Bailey, D.K., Tarney, J., Dunham, K.C., 1980. Isotopic and chemical effects produced in a continuously differentiating convecting Earth mantle. Philosophical transactions of the Royal Society of London. Series A, Math. and Phys. Sci. 297 (1431), 447–477.
Andersen, M.B., Elliott, T., Freymuth, H., Sims, K.W.W., Niu, Y., Kelley, K.A., 2015. The terrestrial uranium isotope cycle. Nature 517 (7534), 356–359.
Andersen, M.B., Vance, D., Morford, J.L., Bura-Nakić, E., Breitenbach, S.F.M., Och, L., 2016. Closing in on the marine $^{238}U/^{235}U$ budget. Chem. Geol. 420, 11–22.
Andersen, M.B., Stirling, C.H., Weyer, S., 2017. Uranium isotope fractionation. In: Teng, F.Z., Watkins, J.M., Dauphas, N. (Eds.), Non-Traditional Stable Isotopes. Reviews in Mineralogy and Geochemistry, pp. 799–850.
Archer, C., Vance, D., 2008. The isotopic signature of the global riverine molybdenum flux and anoxia in the ancient oceans. Nat. Geosci. 1 (9), 597–600.
Arndt, N.T., Goldstein, S.L., 1989. An open boundary between lower continental crust and mantle: its role in crust formation and crustal recycling. Tectonophysics 161, 201–212.
Asael, D., Tissot, F., Reinhard, C.T., Rouxel, O., Dauphas, N., Lyons, T.W., Ponzevera, E., Liorzou, C., Cheron, S., 2013. Coupled molybdenum, iron and uranium stable isotopes as oceanic paleoredox proxies during the Paleoproterozoic Shunga Event. Chem. Geol. 362 (0), 193–210.
Avanzinelli, R., Casalini, M., Elliot, T., Conticelli, S., 2018. Carbon fluxes from subducted carbonates revealed by uranium excess at Mount Vesuvius, Italy. Geology 46 (3), 259–262.
Azrieli-Tal, I., Matthews, A., Bar-Matthews, M., Almogi-Labin, A., Vance, D., Archer, C., Teutsch, N., 2014. Evidence from molybdenum and iron isotopes and molybdenum–uranium covariation for sulphidic bottom waters during Eastern Mediterranean sapropel S1 formation. Earth Planet. Sci. Lett. 393, 231–242.
Bacon, M.P., 1978. Radioactive disequilibrium in altered mid-oceanic basalts. Earth Planet. Sci. Lett. 39 (2), 250–254.
Barling, J., Anbar, A.D., 2004. Molybdenum isotope fractionation during adsorption by manganese oxides. Earth Planet. Sci. Lett. 217 (3–4), 315–329.
Barling, J., Arnold, G.L., Anbar, A.D., 2001. Natural mass-dependent variations in the isotopic composition of molybdenum. Earth Planet. Sci. Lett. 193 (3–4), 447–457.
Bezard, R., Fischer-Gödde, M., Hamelin, C., Brennecka, G.A., Kleine, T., 2016. The effects of magmatic processes and crustal recycling on the molybdenum stable isotopic composition of Mid-Ocean Ridge Basalts. Earth Planet. Sci. Lett. 453, 171–181.
Blusztajn, J., Nielsen, S.G., Marschall, H.R., Shu, Y., Ostrander, C.M., Hanyu, T., 2018. Thallium isotope systematics in volcanic rocks from St. Helena – Constraints on the origin of the HIMU reservoir. Chem. Geol. 476, 292–301.
Burkhardt, C., Hin, R.C., Kleine, T., Bourdon, B., 2014. Evidence for Mo isotope fractionation in the solar nebula and during planetary differentiation. Earth Planet. Sci. Lett. 391, 201–211.
Cabral, R.A., Jackson, M.G., Rose-Koga, E.F., Koga, K.T., Whitehouse, M.J., Antonelli, M. A., Farquhar, J., Day, J.M.D., Hauri, E.H., 2013. Anomalous Sulphur isotopes in plume lavas reveal deep mantle storage of Archaean crust. Nature 496 (7446), 490–493.
Casalini, M., Avanzinelli, R., Tommasini, S., Elliott, T., Conticelli, S., 2019. Ce/Mo and Molybdenum Isotope Systematics in Subduction-Related Orogenic Potassic Magmas of Central-Southern Italy. Geochem. Geophys. Geosyst. 20 (6), 2753–2768.
Castillo, P.R., 2015. The recycling of marine carbonates and sources of HIMU and FOZO Ocean island basalts. Lithos 216–217, 254–263.
Chabaux, F., Riotte, J., Dequincey, O., 2003. U-Th-Ra Fractionation during weathering and river transport. Rev. Mineral. Geochem. 52 (1), 533–576.
Chase, C.G., 1981. Oceanic island Pb: Two-stage histories and mantle evolution. Earth Planet. Sci. Lett. 52 (2), 277–284.
Chauvel, C., Hofmann, A.W., Vidal, P., 1992. HIMU-EM: the French Polynesian connection. Earth Planet. Sci. Lett. 110 (1–4), 99–119.
Chen, S., Hin, R.C., John, T., Brooker, R., Bryan, B., Niu, Y., Elliott, T., 2019. Molybdenum systematics of subducted crust record reactive fluid flow from underlying slab serpentine dehydration. Nat. Commun. 10 (1), 4773.
Delavault, H., Chauvel, C., Sobolev, A., Batanova, V., 2015. Combined petrological, geochemical and isotopic modeling of a plume source: example of Gambier Island, Pitcairn chain. Earth Planet. Sci. Lett. 426 (0), 23–35.
Delavault, H., Chauvel, C., Thomassot, E., Devey, C.W., Dazas, B., 2016. Sulfur and lead isotopic evidence of relic Archean sediments in the Pitcairn mantle plume. Proc. Natl. Acad. Sci. 113 (46), 12952–12956.
Eisele, J., Sharma, M., Galer, S.J.G., Blichert-Toft, J., Devey, C.W., Hofmann, A.W., 2002. The role of sediment recycling in EM-1 inferred from Os, Pb, Hf, Nd, Sr isotope and trace element systematics of the Pitcairn hotspot. Earth Planet. Sci. Lett. 196 (3), 197–212.
Freymuth, H., Vils, F., Willbold, M., Taylor, R.N., Elliott, T., 2015. Molybdenum mobility and isotopic fractionation during subduction at the Mariana arc. Earth Planet. Sci. Lett. 432, 176–186.
Freymuth, H., Elliott, T., van Soest, M., Skora, S., 2016. Tracing subducted black shales in the Lesser Antilles arc using molybdenum isotope ratios. Geology 44 (12), 987–990.
Freymuth, H., Andersen, M.B., Elliott, T., 2019. Uranium isotope fractionation during slab dehydration beneath the Izu arc. Earth Planet. Sci. Lett. 522, 244–254.
Garapić, G., Jackson, M.G., Hauri, E.H., Hart, S.R., Farley, K.A., Blusztajn, J.S., Woodhead, J.D., 2015. A radiogenic isotopic (He-Sr-Nd-Pb-Os) study of lavas from the Pitcairn hotspot: Implications for the origin of EM-1 (enriched mantle 1). Lithos 228–229 (0), 1–11.
Gaschnig, R.M., Reinhard, C.T., Planavsky, N.J., Wang, X., Asael, D., Chauvel, C., 2017. The molybdenum isotope system as a tracer of slab input in subduction zones: an example from Martinique, Lesser Antilles arc. Geochem. Geophys. Geosyst. 18 (12), 4674–4689.
Gaschnig, R.M., Rader, S.T., Reinhard, C.T., Owens, J.D., Planavsky, N., Wang, X., Asael, D., Greaney, A., Helz, R., 2021. Behavior of the Mo, Tl, and U isotope systems during differentiation in the Kilauea Iki lava lake. Chem. Geol. 574, 120239.
Gilleaudeau, G.J., Romaniello, S.J., Luo, G., Kaufman, A.J., Zhang, F., Klaebe, R.M., Kah, L.C., Azmy, K., Bartley, J.K., Zheng, W., Knoll, A.H., Anbar, A.D., 2019. Uranium isotope evidence for limited euxinia in mid-Proterozoic oceans. Earth Planet. Sci. Lett. 521, 150–157.
Goldberg, T., Gordon, G., Izon, G., Archer, C., Pearce, C.R., McManus, J., Anbar, A.D., Rehkamper, M., 2013. Resolution of inter-laboratory discrepancies in Mo isotope data: an intercalibration. J. Analyt. Atom. Spectrom. 28 (5), 724–735.
Graham, D.W., Humphris, S.E., Jenkins, W.J., Kurz, M.D., 1992. Helium isotope geochemistry of some volcanic rocks from Saint Helena. Earth Planet. Sci. Lett. 110 (1), 121–131.

Greaney, A.T., Rudnick, R.L., Helz, R.T., Gaschnig, R.M., Piccoli, P.M., Ash, R.D., 2017. The behavior of chalcophile elements during magmatic differentiation as observed in Kilauea Iki lava lake, Hawaii. Geochim. Cosmochim. Acta 210, 71–96.
Greaney, A.T., Rudnick, R.L., Romaniello, S.J., Johnson, A.C., Anbar, A.D., Cummings, M.L., 2021. Assessing molybdenum isotope fractionation during continental weathering as recorded by weathering profiles in saprolites and bauxites. Chem. Geol. 566, 120103.
Hanyu, T., Kawabata, H., Tatsumi, Y., Kimura, J.-I., Hyodo, H., Sato, K., Miyazaki, T., Chang, Q., Hirahara, Y., Takahashi, T., Senda, R., Nakai, S.i., 2014. Isotope evolution in the HIMU reservoir beneath St. Helena: Implications for the mantle recycling of U and Th. Geochim. Cosmochim. Acta 143, 232–252.
Hart, S.R., Jackson, M.G., 2014. Ta'u and Ofu/Olosega volcanoes: the "Twin Sisters" of Samoa, their P, T, X melting regime, and global implications. Geochem. Geophys. Geosyst. 15 (6), 2301–2318.
Hart, S.R., Hauri, E.H., Oschmann, L.A., Whitehead, J.A., 1992. Mantle Plumes and Entrainment: Isotopic evidence. Science 256 (5056), 517–520.
Hiess, J., Condon, D.J., McLean, N., Noble, S.R., 2012. 238U/235U Systematics in Terrestrial Uranium-Bearing Minerals. Science 335 (6076), 1610–1614.
Hin, R.C., Burkhardt, C., Schmidt, M.W., Bourdon, B., Kleine, T., 2013. Experimental evidence for Mo isotope fractionation between metal and silicate liquids. Earth Planet. Sci. Lett. 379, 38–48.
Hofmann, A.W., 1997. Mantle geochemistry: the message from oceanic volcanism. Nature 385 (6613), 219–229.
Horan, K., Hilton, R.G., McCoy-West, A.J., Selby, D., Tipper, E.T., Hawley, S., Burton, K. W., 2020. Unravelling the controls on the molybdenum isotope ratios of river waters. Geochem. Perspectiv. Lett. 13, 1–6.
Jackson, M.G., Hart, S.R., Koppers, A.A.P., Staudigel, H., Konter, J., Blusztajn, J., Kurz, M., Russell, J.A., 2007a. The return of subducted continental crust in Samoan lavas. Nature 448 (7154), 684–687.
Jackson, M.G., Kurz, M.D., Hart, S.R., Workman, R.K., 2007b. New Samoan lavas from Ofu Island reveal a hemispherically heterogeneous high 3He/4He mantle. Earth Planet. Sci. Lett. 264 (3–4), 360–374.
Jackson, M.G., Hart, S.R., Konter, J.G., Kurz, M.D., Blusztajn, J., Farley, K.A., 2014. Helium and lead isotopes reveal the geochemical geometry of the Samoan plume. Nature 514 (7522), 355–358.
Johnson, D.M., Hooper, P.R., Conrey, R.M., 1999. XRF analysis of rocks and minerals for major and trace elements on a single low dilution Li-tetraborate fused bead. Adv. X-ray Anal. 41, 843–867.
Kawabata, H., Hanyu, T., Chang, Q., Kimura, J.-I., Nichols, A.R.L., Tatsumi, Y., 2011. The Petrology and Geochemistry of St. Helena Alkali Basalts: Evaluation of the Oceanic Crust-recycling Model for HIMU OIB. J. Petrol. 52 (4), 791–838.
Kay, R.W., Mahlburg-Kay, S., 1991. Creation and destruction of lower continental crust. Geol. Rundsch. 80, 259–278.
Kendall, B., Gordon, G.W., Poulton, S.W., Anbar, A.D., 2011. Molybdenum isotope constraints on the extent of late Paleoproterozoic Ocean euxinia. Earth Planet. Sci. Lett. 307 (3), 450–460.
Kendall, B., Dahl, T.W., Anbar, A.D., 2017. The stable isotope geochemistry of molybdenum. In: Watkins, J., Dauphas, N. (Eds.), Teng, F.Z. Non-Traditional Stable Isotopes. Reviews in Mineralogy and Geochemistry, Mineralogical Society of America and Geochemical Society, pp. 683–732.
Kimura, J.-I., Gill, J.B., Skora, S., van Keken, P.E., Kawabata, H., 2016. Origin of geochemical mantle components: Role of subduction filter. Geochem. Geophys. Geosyst. 17 (8), 3289–3325.
King, E.K., Pett-Ridge, J.C., 2018. Reassessing the dissolved molybdenum isotopic composition of ocean inputs: the effect of chemical weathering and groundwater. Geology 46 (11), 955–958.
King, E.K., Thompson, A., Chadwick, O.A., Pett-Ridge, J.C., 2016. Molybdenum sources and isotopic composition during early stages of pedogenesis along a basaltic climate transect. Chem. Geol. 445, 54–67.
Knaack, C., Cornelius, S., Hooper, P.R., 1994. Trace Element Analysis of Rocks and Minerals by ICP-MS. Department of Geology, Washington State University, Open File Report.
König, S., Wille, M., Voegelin, A., Schoenberg, R., 2016. Molybdenum isotope systematics in subduction zones. Earth Planet. Sci. Lett. 447, 95–102.
Koppers, A.A.P., Russell, J.A., Roberts, J., Jackson, M.G., Konter, J.G., Wright, D.J., Staudigel, H., Hart, S.R., 2011. Age systematics of two young en echelon Samoan volcanic trails. Geochem. Geophys. Geosyst. 12, 2010GC003438.
Li, J., Zhu, X.-k., Tang, S.-h., Zhang, K., 2016. High-Precision Measurement of Molybdenum Isotopic Compositions of selected Geochemical Reference Materials. Geostand. Geoanal. Res. 40 (3), 405–415.
Li, J., Liang, X.-R., Zhong, L.-F., Wang, X.-C., Ren, Z.-Y., Sun, S.-L., Zhang, Z.-F., Xu, J.-F., 2014. Measurement of the Isotopic Composition of Molybdenum in Geological Samples by MC-ICP-MS using a Novel Chromatographic Extraction Technique. Geostand. Geoanal. Res. 38 (3), 345–354.
Liang, Y.-H., Halliday, A.N., Siebert, C., Fitton, J.G., Burton, K.W., Wang, K.-L., Harvey, J., 2017. Molybdenum isotope fractionation in the mantle. Geochim. Cosmochim. Acta 199, 91–111.
Liermann, L.J., Mathur, R., Wasylenki, L.E., Nuester, J., Anbar, A.D., Brantley, S.L., 2011. Extent and isotopic composition of Fe and Mo release from two Pennsylvania shales in the presence of organic ligands and bacteria. Chem. Geol. 281 (3), 167–180.
Liu, X.-M., Teng, F.-Z., Rudnick, R.L., McDonough, W.F., Cummings, M.L., 2014. Massive magnesium depletion and isotope fractionation in weathered basalts. Geochim. Cosmochim. Acta 135 (0), 336–349.
Liu, J.-H., Zhou, L., Algeo, T.J., Wang, X.-C., Wang, Q., Wang, Y., Chen, M.-L., 2020. Molybdenum isotopic behavior during intense weathering of basalt on Hainan Island, South China. Geochim. Cosmochim. Acta 287, 180–204.
Livermore, B.D., Connelly, J.N., Moynier, F., Bizzarro, M., 2018. Evaluating the robustness of a consensus 238U/235U value for U-Pb geochronology. Geochim. Cosmochim. Acta 237, 171–183.
MacDougall, J.D., Finkel, R.C., Carlson, J., Krishnaswami, S., 1979. Isotopic evidence for uranium exchange during low-temperature alteration of oceanic basalt. Earth Planet. Sci. Lett. 42 (1), 27–34.
McCoy-West, A.J., Chowdhury, P., Burton, K.W., Sossi, P., Nowell, G.M., Fitton, J.G., Kerr, A.C., Cawood, P.A., Williams, H.M., 2019. Extensive crustal extraction in Earth's early history inferred from molybdenum isotopes. Nat. Geosci. 12 (11), 946–951.
McDougall, I.A.N., 2010. Age of volcanism and its migration in the Samoa Islands. Geol. Mag. 147, 705–717.
McManus, J., Nägler, T.F., Siebert, C., Wheat, C.G., Hammond, D.E., 2002. Oceanic molybdenum isotope fractionation: Diagenesis and hydrothermal ridge-flank alteration. Geochemistry, Geophysics, Geosystems 3 (12), 1078.
Montoya-Pino, C., Weyer, S., Anbar, A.D., Pross, J., Oschmann, W., van de Schootbrugge, B., Arz, H.W., 2010. Global enhancement of ocean anoxia during Oceanic Anoxic Event 2: A quantitative approach using U isotopes. Geology 38 (4), 315–318.
Moreira-Nordemann, L.M., 1980. Use of 234U/238U disequilibrium in measuring chemical weathering rate of rocks. Geochim. Cosmochim. Acta 44 (1), 103–108.
Nägler, T.F., Anbar, A.D., Archer, C., Goldberg, T., Gordon, G.W., Greber, N.D., Siebert, C., Sohrin, Y., Vance, D., 2014. Proposal for an International Molybdenum Isotope Measurement Standard and Data Representation. Geostand. Geoanal. Res. 38 (2), 149–151.
Nesbitt, H.W., Young, G.M., 1982. Early Proterozoic climates and plate motions inferred from major element chemistry of lutites. Nature 299, 715–717.
Nesbitt, H.W., Young, G.M., 1984. Prediction of some weathering trends of plutonic and volcanic rocks based on thermodynamic and kinetic considerations. Geochim. Cosmochim. Acta 48 (7), 1523–1534.
Newsom, H.E., Palme, H., 1984. The depletion of siderophile elements in the Earth's mantle: new evidence from molybdenum and tungsten. Earth Planet. Sci. Lett. 69 (2), 354–364.
Newsom, H.E., White, W.M., Jochum, K.P., Hofmann, A.W., 1986. Siderophile and chalcophile element abundances in oceanic basalts, Pb isotope evolution and growth of the Earth's core. Earth Planet. Sci. Lett. 80 (3), 299–313.
Noordmann, J., Weyer, S., Georg, R.B., Jöns, S., Sharma, M., 2015. 238U/235U isotope ratios of crustal material, rivers and products of hydrothermal alteration: new insights on the oceanic U isotope mass balance. Isot. Environ. Health Stud. 1–23.
Ohta, T., Arai, H., 2007. Statistical empirical index of chemical weathering in igneous rocks: A new tool for evaluating the degree of weathering. Chem. Geol. 240 (3–4), 280–297.
Partin, C.A., Bekker, A., Planavsky, N.J., Lyons, T.W., 2015. Euxinic conditions recorded in the ca. 1.93 Ga Bravo Lake Formation, Nunavut (Canada): Implications for oceanic redox evolution. Chem. Geol. 417, 148–162.
Pearce, C.R., Burton, K.W., von Strandmann, P.A.E.P., James, R.H., Gislason, S.R., 2010. Molybdenum isotope behaviour accompanying weathering and riverine transport in a basaltic terrain. Earth Planet. Sci. Lett. 295 (1–2), 104–114.
Planavsky, N.J., Reinhard, C.T., Wang, X., Thomson, D., McGoldrick, P., Rainbird, R.H., Johnson, T., Fischer, W.W., Lyons, T.W., 2014. Low Mid-Proterozoic atmospheric oxygen levels and the delayed rise of animals. Science 346 (6209), 635–638.
Sarin, M.M., Krishnaswami, S., somayajulu, B.L.K., Moore, W.S., 1990. Chemistry of uranium, thorium, and radium isotopes in the Ganga-Brahmaputra river system: Weathering processes and fluxes to the Bay of Bengal. Geochim. Cosmochim. Acta 54 (5), 1387–1396.
Sims, K.W.W., Hart, S.R., Reagan, M.K., Blusztajn, J., Staudigel, H., Sohn, R.A., Layne, G. D., Ball, L.A., Andrews, J., 2008. 238U-230Th-226Ra-210Pb-210Po, 232Th-228Ra, and 235U-231Pa constraints on the ages and petrogenesis of Vailulu'u and Malumalu Lavas, Samoa. Geochem. Geophys. Geosyst. 9 (4).
Skora, S., Freymuth, H., Blundy, J., Elliott, T., Guillong, M., 2017. An experimental study of the behaviour of cerium/molybdenum ratios during subduction: Implications for tracing the slab component in the Lesser Antilles and Mariana Arc. Geochim. Cosmochim. Acta 212, 133–155.
Stirling, C.H., Andersen, M.B., Potter, E.-K., Halliday, A.N., 2007. Low-temperature isotopic fractionation of uranium. Earth Planet. Sci. Lett. 264 (1–2), 208–225.
Stracke, A., Bizimis, M., Salters, V.J.M., 2003. Recycling oceanic crust: Quantitative constraints. Geochem. Geophys. Geosyst. 4 (3).
Stracke, A., Hofmann, A.W., Hart, S.R., 2005. FOZO, HIMU, and the rest of the mantle zoo. Geochem. Geophys. Geosyst. 6 (5).
Telus, M., Dauphas, N., Moynier, F.D.R., Tissot, F.O.L.H., Teng, F.-Z., Nabelek, P.I., Craddock, P.R., Groat, L.A., 2012. Iron, zinc, magnesium and uranium isotopic fractionation during continental crust differentiation: the tale from migmatites, granitoids, and pegmatites. Geochim. Cosmochim. Acta 97 (0), 247–265.
Teng, F.Z., Li, W.Y., Rudnick, R.L., Gardner, L.R., 2010. Contrasting lithium and magnesium isotope fractionation during continental weathering. Earth Planet. Sci. Lett. 300 (1–2), 63–71.
Thurber, D.L., 1962. Anomalous U234 U238 in nature. J. Geophys. Res. (1896–1977) 67 (11), 4518–4520.
Tissot, F.L.H., Dauphas, N., 2015. Uranium isotopic compositions of the crust and ocean: Age corrections, U budget and global extent of modern anoxia. Geochim. Cosmochim. Acta 167, 113–143.
Tissot, F.L.H., Ibanez-Mejia, M., Boehnke, P., Dauphas, N., McGee, D., Grove, T.L., Harrison, T.M., 2019. 238U/235U measurement in single-zircon crystals: implications for the Hadean environment, magmatic differentiation and geochronology. J. Anal. At. Spectrom. 34 (10), 2035–2052.

Villalobos-Orchard, J., Freymuth, H., O'Driscoll, B., Elliott, T., Williams, H., Casalini, M., Willbold, M., 2020. Molybdenum isotope ratios in Izu arc basalts: the control of subduction zone fluids on compositional variations in arc volcanic systems. Geochim. Cosmochim. Acta 288, 68–82.
Voegelin, A.R., Nagler, T.F., Pettke, T., Neubert, N., Steinmann, M., Pourret, O., Villa, I. M., 2012. The impact of igneous bedrock weathering on the Mo isotopic composition of stream waters: Natural samples and laboratory experiments. Geochim. Cosmochim. Acta 86, 150–165.
Voegelin, A.R., Pettke, T., Greber, N.D., von Niederhäusern, B., Nägler, T.F., 2014. Magma differentiation fractionates Mo isotope ratios: evidence from the Kos Plateau Tuff (Aegean Arc). Lithos 190–191, 440–448.
Wang, Z., Ma, J., Li, J., Zeng, T., Zhang, Z., He, X., Zhang, L., Wei, G., 2020. Effect of Fe–Ti oxides on Mo isotopic variations in lateritic weathering profiles of basalt. Geochim. Cosmochim Acta 286, 380–403.
Wang, X., Planavsky, N.J., Reinhard, C.T., Hein, J.R., Johnson, T.M., 2016. A Cenozoic seawater redox record derived from 238U/235U in ferromanganese crusts. Am. J. Sci. 316 (1), 64–83.
Weis, D., Kieffer, B., Maerschalk, C., Pretorius, W., Barling, J., 2005. High-precision Pb-Sr-Nd-Hf isotopic characterization of USGS BHVO-1 and BHVO-2 reference materials. Geochem. Geophys. Geosyst. 6 (2). Q02002.
Weis, D., Kieffer, B., Maerschalk, C., Barling, J., de Jong, J., Williams, G.A., Hanano, D., Pretorius, W., Mattielli, N., Scoates, J.S., Goolaerts, A., Friedman, R.M., Mahoney, J. B., 2006. High-precision isotopic characterization of USGS reference materials by TIMS and MC-ICP-MS. Geochem. Geophys. Geosyst. 7 (8). Q08006.
Weiss, Y., Class, C., Goldstein, S.L., Hanyu, T., 2016. Key new pieces of the HIMU puzzle from olivines and diamond inclusions. Nature 537, 666–670.
Weyer, S., Anbar, A.D., Gerdes, A., Gordon, G.W., Algeo, T.J., Boyle, E.A., 2008. Natural fractionation of 238U/235U. Geochim. Cosmochim. Acta 72 (2), 345–359.
White, W.M., 1985. Sources of oceanic basalts: Radiogenic isotopic evidence. Geology 13 (2), 115–118.
White, W.M., 2010. Oceanic Island Basalts and Mantle Plumes: the Geochemical Perspective. Annu. Rev. Earth Planet. Sci. 38 (1), 133–160.
White, W.M., Hofmann, A.W., 1982. Sr and Nd isotope geochemistry of oceanic basalts and mantle evolution. Nature 296 (5860), 821–825.
Wiederhold, J.G., Teutsch, N., Kraemer, S.M., Halliday, A.N., Kretzschmar, R., 2007. Iron isotope fractionation in oxic soils by mineral weathering and podzolization. Geochim. Cosmochim. Acta 71 (23), 5821–5833.
Willbold, M., Elliott, T., 2017. Molybdenum isotope variations in magmatic rocks. Chem. Geol. 449, 253–268.
Willbold, M., Hibbert, K., Lai, Y.-J., Freymuth, H., Hin, R.C., Coath, C., Vils, F., Elliott, T., 2016. High-precision mass-dependent Molybdenum Isotope variations in Magmatic Rocks determined by Double-Spike MC-ICP-MS. Geostand. Geoanalyt. Res. 40 (3), 389–403.
Willbold, M., Stracke, A., 2010. Formation of enriched mantle components by recycling of upper and lower continental crust. Chem. Geol. 276 (3), 188–197.
Willbold, M., Elliott, T., Archer, C., 2012. Mass-dependent molybdenum isotope variations in ocean island basalts. Mineral. Mag. 76, 2546.
Wille, M., Nebel, O., Pettke, T., Vroon, P.Z., König, S., Schoenberg, R., 2018. Molybdenum isotope variations in calc-alkaline lavas from the Banda arc, Indonesia: Assessing the effect of crystal fractionation in creating isotopically heavy continental crust. Chem. Geol. 485, 1–13.
Woodhead, J.D., 1996. Extreme HIMU in an oceanic setting: the geochemistry of Mangaia Island (Polynesia), and temporal evolution of the Cookâ€Austral hotspot. J. Volcanol. Geotherm. Res. 72, 1–19.
Woodhead, J., McCulloch, M.T., 1989. Ancient seafloor signals in Pitcairn Island lavas and evidence for large amplitude, small length-scale mantle heterogeneities. Earth Planet. Sci. Lett. 94, 257–273.
Workman, R.K., Hart, S.R., Jackson, M., Regelous, M., Farley, K.A., Blusztajn, J., Kurz, M., Staudigel, H., 2004. Recycled metasomatized lithosphere as the origin of the Enriched Mantle II (EM2) end-member: Evidence from the Samoan Volcanic Chain. Geochem. Geophys. Geosyst. 5 (4). Q04008.
Workman, R.K., Eiler, J.M., Hart, S.R., Jackson, M.G., 2008. Oxygen isotopes in Samoan lavas: Confirmation of continent recycling. Geology 36, 551–554.
Yang, J., Siebert, C., Barling, J., Savage, P., Liang, Y.-H., Halliday, A.N., 2015. Absence of molybdenum isotope fractionation during magmatic differentiation at Hekla volcano, Iceland. Geochim. Cosmochim. Acta 162, 126–136.
Yang, J., Barling, J., Siebert, C., Fietzke, J., Stephens, E., Halliday, A.N., 2017. The molybdenum isotopic compositions of I-, S- and A-type granitic suites. Geochim. Cosmochim. Acta 205, 168–186.
Zhao, P.-P., Li, J., Zhang, L., Wang, Z.-B., Kong, D.-X., Ma, J.-L., Wei, G.-J., Xu, J.-F., 2016. Molybdenum Mass Fractions and Isotopic Compositions of International Geological Reference Materials. Geostand. Geoanal. Res. 40 (2), 217–226.
Zindler, A., Hart, S., 1986. Chemical Geodynamics. Annu. Rev. Earth Planet. Sci. 14 (1), 493–571.